

Pentagram Rigidity for Centrally Symmetric Octagons

Richard Evan Schwartz *

November 25, 2021

Abstract

In this paper I will establish a special case of a conjecture that intertwines the deep diagonal pentagram maps and Poncelet polygons. The special case is that of the 3-diagonal map acting on affine equivalence classes of centrally symmetric octagons. This is the simplest case that goes beyond an analysis of elliptic curves. The proof involves establishing that the map is Arnold-Liouville integrable in this case, and then exploring the Lagrangian surface foliation in detail.

1 Introduction

1.1 Conjecture and Results

A *Poncelet polygon* in the projective plane is one whose vertices lie in one conic section and whose edges lie in lines tangent to another conic section. A polygon in the projective plane is *convex* if it is convex in the ordinary sense when viewed in an affine patch. (See §2.1 for definitions.) In an affine patch, a convex Poncelet polygon is inscribed in one ellipse and circumscribed about another.

Let (n, k) be relatively prime integers with $n \geq 7$ and $k \in (2, n/2)$. Given an n -gon P_1 , we let $P_2 = T_k(P_1)$ be the n -gon obtained by intersecting the successive k -diagonals of P_1 . Figure 1 shows this for $(n, k) = (8, 3)$. The map T_k is generically defined and invertible. The same construction works

*Supported by N.S.F. Grant DMS-2102802

in any field, but the concept of convexity, which requires the real numbers, is important for us here. The maps T_k and T_k^{-1} are always defined on convex n -gons, though the image of a convex n -gon under one of these maps need not be convex. Figure 1 (right) gives an example where P_1 is convex but P_2 is not.

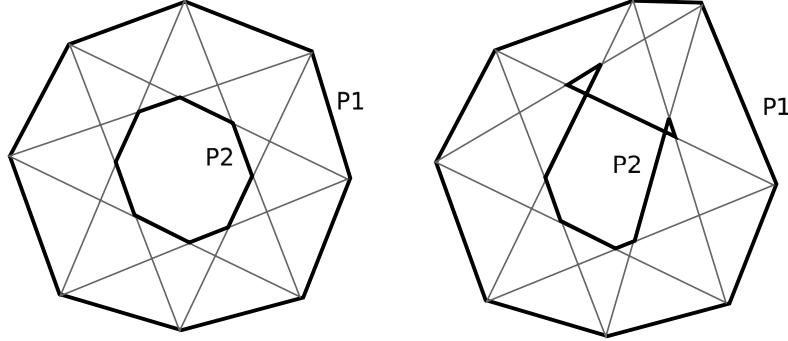


Figure 1: P_1 and $P_2 = T_3(P_1)$.

Starting with P_0 we define the k -pentagram orbit to be the bi-infinite sequence $\{P_j\}$ where $P_j = T_k^j(P_0)$.

Conjecture 1.1 *Let P_0 be a convex n -gon and let $\{P_j\}$ be its k -pentagram orbit. If $\{P_j\}$ is convex for all $j \in \mathbf{Z}$ then P_0 is Poncelet.*

Remarks:

- (1) In [16] I proved that if P is Poncelet then $T_k(P)$ and P are projectively equivalent. This implies the converse of the conjecture: If P_0 is convex Poncelet then $\{P_n\}$ is convex for all n . Thus, the conjecture above implies that $\{P_n\}$ is convex for all n if and only if P_0 is convex Poncelet.
- (2) The restriction that n and k are relatively prime is probably not strictly necessary, but the result can fail when n and k are both even. I don't know the exact restrictions needed.
- (3) The image of a convex n -gon under T_2 or T_2^{-1} is always convex in the projective plane. Here T_2 is also called the *pentagram map*, and it has been studied extensively.

In [17] I proved Conjecture 1.1 for the case of 8-gons with 4-fold rotational symmetry. In this toy case, the moduli space is foliated by T_3 invariant elliptic curves. I worked this case out as a proof of concept. In this paper I will prove

the first really nontrivial case of the conjecture, a case that goes beyond the analysis of elliptic curves. An even-sided polygon P is *centrally symmetric* if it is invariant with respect to the map $p \rightarrow -p$. The Poncelet polygons with an even number of sides are always centrally symmetric. See [4].

Theorem 1.2 (Main) *Let P_0 be a convex centrally symmetric 8-gon and $\{P_k\}$ its 3-pentagram orbit. If P_j is convex for all $j \in \mathbf{Z}$ then P_0 is Poncelet.*

In §9, when we treat the case of inscribed and circumscribed 8-gons, we will obtain further structural results. Let \mathcal{CI}^* denote the space of affine equivalence classes of convex centrally symmetric 8-gons which are circumscribed in ellipses.

Theorem 1.3 *The set \mathcal{CI}^* is forward invariant, and for every $\xi \in \mathcal{CI}^*$ the following is true:*

- $T_3^n(\xi)$ converges to the affine equivalence class of a convex Poncelet 8-gon as $n \rightarrow +\infty$.
- $T_n^{-n}(\xi)$ converges to the affine equivalence class of a star-convex Poncelet 8-gon as $n \rightarrow +\infty$ provided that these images are all well-defined.

Remarks:

- (1) A dual result holds for the space \mathcal{CI} of affine classes of centrally symmetric inscribed 8-gons. All that changes in the statement is that T_3 and T_3^{-1} are swapped.
- (2) For generic choices of ξ the backwards iterates $T_3^{-n}(\xi)$ will be everywhere defined. However, for some special choices this might not be the case.
- (3) In [18], Serge Tabachnikov and I show, among various results, that when ξ is any inscribed 8-gon (not necessarily convex) the iterate $T_3(\xi)$ is also inscribed. Dually, the same holds when *circumscribed* replaces *inscribed*. Theorem 1.3 is an enhancement of this result in [18].

Theorem 1.3 is really the easy part of the analysis. The much more difficult and interesting part is the case of 8-gons which are neither inscribed nor circumscribed in conics. Let $\mathcal{P}_{8,2}$ denote the space of affine classes of centrally symmetric 8-gons. One of the key steps we use in dealing with this case is the following integrability result. (See §2.2 for definitions.)

Theorem 1.4 *The action of T_3 on $\mathcal{P}_{8,2}$ has an invariant (singular) symplectic form and 2 algebraically independent rational invariants which Poisson commute with respect to it.*

1.2 Context

Here is an abbreviation of the discussion in [17]. The pentagram map, T_2 , is one of the best known discrete completely integrable system. See for instance, [1], [2], [3], [8], [9], [10], [11], [12], [14], [15], [20], [21]. The Pentagram Rigidity Conjecture *would be* a statement about the global topology of an abelian foliation associated to a completely integrable system if the map T_3 were known to be completely integrable.

A kind of complete integrability is known for T_k for all $k \geq 2$. It is proved in [3] that T_k is completely integrable when defined on the space of *twisted, corrugated* polygons. Corrugated polygons are higher dimensional polygons which satisfy the incidence relations needed to make T_k well-defined. (Beautifully, this property is preserved by T_k .) Twisted n -gons are maps of \mathbf{Z} into projective space which have the property that $\Psi(n+k) = \Gamma \circ \Psi(k)$ for all k and for some projective transformation Γ . So far, nobody has used the work in [3] to establish the complete integrability of T_k for ordinary polygons, though experts think that perhaps this is possible to do.

Theorem 1.4 gives a positive answer to the integrability question about T_3 in the first really nontrivial case. T_3 is indeed completely integrable in the Arnold-Liouville sense, on $\mathcal{P}_{8,2}$. One fine point is that the invariant symplectic form has poles along the coordinate hyperplanes, though the associated invariant Poisson structure is still well defined there. I found the invariant symplectic form on $\mathcal{P}_{8,2}$, as well as the two invariant quantities, by inspired guesswork. I did not try to use the various machines that are now known to work with T_2 – e.g., cluster algebras, refactorings, Lax pairs, the Kenyon-Goncharov dimer systems, and spin networks.

Theorem 1.2 involves an analysis of the geometry and topology of the level sets of the invariants. The essential point is that the level sets which intersect the subspace of $\mathcal{P}_{8,2}$ containing the convex polygons also contain points outside this space. The dynamics on these level sets, thanks to the complete integrability (and a lot of hard work) is essentially torus motion, and it mixes up the subset of convex points with the subset of non-convex points unless the starting point represents a Poncelet 8-gon.

It is surprising to me that this integrable structure coexists with the hyperbolic behavior seen in Theorem 1.3, but there is no contradiction here. This sort of coexistence also appears e.g. in the phase space of elliptical billiards. We have a higher dimensional analogue of the same phenomenon.

1.3 Pictures of Orbits

I spent much time drawing pictures of the orbits of T_3 . Let me share two of them. Figure 2 (left) shows a planar projection of the first 2^{15} points of an orbit that starts with a convex point. (A *convex point* is one that represents a convex 8-gon.) We will prove that such level sets are finite unions of cylinders and disks, and the metric completion (with respect to the flat metrics coming from the integrable structure) is a smooth flat torus. Thinking extrinsically, in terms of the subset of \mathbf{R}^4 , this metric completion operation is very closely related to blowing up at certain points. The darkly shaded part of the orbit is the set of convex points it contains. So, in this case, most of the orbit lies outside the locus of convex points and it is pretty clear that the action of T_3 mixes things as I have described.

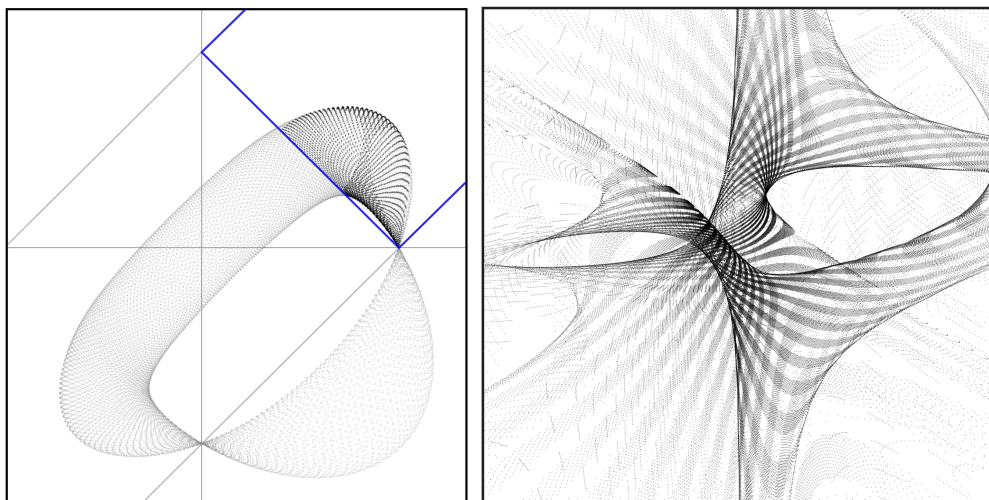


Figure 2: A torus orbit and a beautiful orbit.

Figure 2 (right) shows a planar projection of the first 2^{19} points of an orbit that does not contain any convex points. This kind of orbit is irrelevant to our analysis but I can't resist showing it. I think that this surface has higher genus, and that the complete integrability imparts a singular flat structure on it. The singular nature of the various objects involved allows for these higher genus orbit closures. Notice that the surface appears to have higher genus but nonetheless seems to have orbits which fill it out in a very structured way. I have not studied these orbits carefully yet but intend to.

1.4 Organization

In §2 I will give some background information about projective geometry, integrable systems, and a bit of computational algebraic geometry. In §3 I will prove Theorem 1.4. In §3.6 I will give a detailed outline of the proof of Theorem 1.2. In §4-9 I carry out various details of the outline. The final chapter contains the proof of Theorem 1.3.

Why is this paper so long? The complete integrability result has a short proof, but then the challenges begin. One difficulty is that we need to understand *every single orbit* that contains points representing convex 8-gons, so the usual appeal to Sard's Theorem to show that most level sets are smooth will not help us. We need to use some computer algebra for the very exacting requirements of the Rigidity Conjecture. The expressions involved are sometimes enormous.

Even after we know that every relevant orbit is smooth, we have to deal with the fact that the level sets have many components to them because they are divided up by the coordinate hyperplanes. We need to compute the topology of every component and then assemble them. The smoothness and transversality we establish allow for some crucial continuity arguments which control the topology. The final difficulty is that T_3 sometimes blows up or blows down various ends of our level set components. The paper represents the implementation of simple geometric ideas, as described in the outline in §3.6, but the complications just described make the paper very long. I wish it was not the case.

The interested reader can download the computer program I wrote, which does experiments with the 3-diagonal map on centrally symmetric octagons. The location of the program is
<http://www.math.brown.edu/~res/Java/OCTAGON.tar>

1.5 Acknowledgements

I would like to thank Misha Bialy, Dan Cristofaro-Gardiner, Misha Gehkتمان, Anton Izosimov, Curtis McMullen, Valentin Ovsienko, Dan Reznik, Joe Silverman, Sergei Tabachnikov, and Max Weinreich for helpful conversations.

2 Preliminaries

2.1 Projective Geometry

The *real projective plane* \mathbf{RP}^2 is the space of lines through the origin in \mathbf{R}^3 . Equivalently it is the space of scale-equivalence-classes of nonzero vectors in \mathbf{R}^3 . Points in \mathbf{RP}^2 will be denoted by $[x : y : z]$. This point represents the line through the origin and (x, y, z) . The quotient map $\mathbf{R}^3 \rightarrow \mathbf{RP}^2$ is called *projectivization*.

There is a natural inclusion $\mathbf{R}^2 \rightarrow \mathbf{RP}^2$ given by

$$(x, y) \rightarrow [x : y : 1]. \quad (1)$$

The image of this inclusion is known as the *standard affine patch*. I often identify \mathbf{R}^2 with its image under this inclusion, and when speaking about points in the affine patch I will often write (x, y) for $[x : y : 1]$. The inclusion in Equation 1 has an inverse, given by

$$[x : y : z] \rightarrow (x/z, y/z). \quad (2)$$

The *line at infinity* is the subset of \mathbf{RP}^2 outside the standard affine patch. The line at infinity consists of points of the form $[x : y : 0]$. More generally, a *line* in \mathbf{RP}^2 is the set of members represented by lines in a 2-dimensional subspace of \mathbf{R}^3 . We can also represent lines by triples $[a : b : c]$. This point represents the linear subspace given by the equation $ax + by + cz = 0$. An *affine patch* is the complement of a line. A subset of \mathbf{RP}^2 is *convex* if it is contained in an affine patch and is convex in the ordinary sense when that affine patch is identified with \mathbf{R}^2 .

Conveniently, the line through 2 points is represented by the cross product of the corresponding vectors. Likewise, the intersection of 2 lines is given by the cross product of the corresponding vectors. The line containing points represented by $[x_1 : y_1 : z_1]$ and $[x_2 : y_2 : z_2]$ is found by taking the cross product $(x_1, y_1, z_1) \times (x_2, y_2, z_2)$. Dually, the intersection of two lines given by these coordinates is found by taking their cross product. There is a complete symmetry between the two operations. If we have 4 points A, B, C, D then we have

$$\overline{AB} \cap \overline{CD} = (A \times B) \times (C \times D). \quad (3)$$

The equals sign means that the resulting vector on the right represents the point on the left when it is interpreted as a point in the projective plane. Equation 3 makes it easy to compute the map T_3 in coordinates.

2.2 Complete Integrability

Invariant Functions and Level Sets: Let $U \subset V \subset \mathbf{R}^4$ be two open sets and suppose we have a smooth map $T : U \rightarrow V$. Our map T will be a suitable restriction of maps closely related to T_3 , and U, V will be subsets of $\mathcal{P}_{8,2}$, a space we identify with an open dense subset of \mathbf{R}^4 .

Suppose that $F_1, F_2 : V \rightarrow \mathbf{R}$ are two smooth T -invariant functions. The map $\Psi = (F_1, F_2)$ gives us a smooth and T -invariant map from V into \mathbf{R}^2 . We call a pair $(x, y) \in \mathbf{R}^2$ a *regular value* if the gradients ∇F_1 and ∇F_2 are nonzero and linearly independent for all $p \in \Psi^{-1}(x, y)$. Otherwise we call (x, y) a *singular value*. Sard's Theorem guarantees that the set of singular values has measure 0 in \mathbf{R}^2 . When (x, y) is a regular value the level set

$$\Sigma = \Psi^{-1}(x, y) \subset V$$

is a smooth surface. Furthermore $T(\Sigma \cap U) \subset \Sigma$.

Invariant Symplectic Form: We fix some level set Σ and assume it is a regular level set. A *symplectic form* on V is a smooth, closed and non-degenerate 2-form. Let ω be such a form. This form is called *T -invariant* if

$$\omega(dT_p(V), dT_p(W)) = \omega(V, W), \quad \forall V, W \in T_p(U), \quad \forall p \in U.$$

Given ω and F_j , there is a unique vector field X_j such that

$$\omega(X_j, V) = D_V F_j.$$

Here $D_V F_j$ is the directional derivative of F_j in the direction of V . The vector field X_j is called the *Hamiltonian of F_j* . Because $\omega(X_j, X_j) = 0$, the vector field X_j is tangent to the level set of F_j . Also, the flow generated by F_j is symplectic; it preserves ω .

The functions F_1 and F_2 *Poisson commute* if

$$\omega(X_1, X_2) = 0 \tag{4}$$

everywhere. The vectors X_1, X_2 are linearly independent at some point iff the gradients $\nabla F_1, \nabla F_2$ are linearly independent at this point. When this happens, the restriction of ω to Σ is 0. That is, Σ is *Lagrangian*. The vector fields X_1 and X_2 define commuting flows that preserve both Σ and ω .

Translation Surface Structure: We can use these commuting flows to define coordinate charts from Σ into \mathbf{R}^2 in a canonical way. We start with some point $p \in \Sigma$, which we map to the origin. Each point $q \in \Sigma$ sufficiently near to p defines two numbers $a_1(p, q)$ and $a_2(p, q)$ such that one can reach q by starting at p and flowing for time $a_1(p, q)$ along X_1 and then for time $a_2(p, q)$ along F_2 . The coordinate chart is given by

$$q \rightarrow (a_1(p, q), a_2(p, q)).$$

The commuting nature of the flows combines with the linear independence to show that this map really is a local coordinate chart about p .

By construction, the overlap functions for our coordinate chart are translations. Thus Σ has the structure of translation surface (without singular points). Since everything is T -invariant, the map $T : \Sigma \cap U \rightarrow \Sigma$ is a translation in these coordinates. In particular, T is an isometry in these coordinates. In this case we would say that T is *completely integrable* with respect to the pair (U, V) . The complete integrability makes T into a translation on its regular level sets.

Smooth Global Picture: Now we discuss the classical global picture. We don't quite have this situation but it is certainly worth mentioning. The global picture is that $U = V = M$, a compact smooth 4-manifold. In this case, when Σ is a regular level set, it is a finite union of compact surfaces. Each component has a canonical translation structure and therefore must be equivalent to a flat torus. Some power of T preserves each of these flat tori and acts as a translation on it. All this generalizes to higher even dimensional manifolds in a straightforward way.

Rational Global Picture: In our case we have a rational map T on \mathbf{R}^4 and we will construct two invariant rational functions F_1 and F_2 . We also will find a T -invariant and rationally defined symplectic form. All these objects have singularities; they are only defined on open dense subsets of \mathbf{R}^4 . These singularities allow for the kind of higher genus level sets suggested by Figure 2. However, we will always restrict our attention to suitable pairs (U, V) of open sets where everything is everywhere defined. Thus, by restriction, we get back to the clean local picture discussed above.

2.3 Resultants

For ease of typesetting, I will describe the resultant for two polynomials of degree 2 and 3. The construction is meant to work for general polynomials of degree m and n . See §2 of [19] for more details.

Given 2 polynomials

$$P = a_2x^2 + a_1x + a_0, \quad Q = b_3x^3 + b_2x^2 + b_1x + b_0,$$

the *resultant* is defined to be

$$\text{res}(P, Q) = \det \begin{bmatrix} a_2 & a_1 & a_0 & 0 & 0 \\ 0 & a_2 & a_1 & a_0 & 0 \\ 0 & 0 & a_2 & a_1 & a_0 \\ b_3 & b_2 & b_1 & b_0 & 0 \\ 0 & b_3 & b_2 & b_1 & b_0 \end{bmatrix} \quad (5)$$

This number vanishes if and only if P and Q have a common (complex) root.

In the multivariable case, one can treat two polynomials $P(x_1, \dots, x_n)$ and $Q(x_1, \dots, x_n)$ as elements of the ring $R[x_n]$ where $R = \mathbf{C}[x_1, \dots, x_{n-1}]$. The resultant

$$\text{res}(P, Q, x_n) \quad (6)$$

computes the resultant in R and thus gives a polynomial in $\mathbf{C}[x_1, \dots, x_{n-1}]$. The polynomials P and Q simultaneously vanish at (x_1, \dots, x_n) only if the resultant $\text{res}(P, Q, x_n)$ vanishes at (x_1, \dots, x_{n-1}) .

2.4 A Positivity Certificate

Here I'll explain a criterion for when a polynomial is positive on the half-open cube $(0, 1]^n$. Any polynomial $F \in \mathbf{R}[x_1, \dots, x_n]$ can be written succinctly as

$$F = \sum A_I X^I, \quad A_I \in \mathbf{R}, \quad (7)$$

where the sum is taken over all multi-indices. If $I' = (i'_1, \dots, i'_n)$ we write $I' \leq I$ if $i'_j \leq i_j$ for all $j = 1, \dots, n$. We call F *weak positive dominant* if

$$\sum_{I' \leq I} A_{I'} \geq 0 \quad \forall I. \quad (8)$$

We call F *positive dominant* if F is weak positive dominant and additionally the sum of all the coefficients of F is positive.

Lemma 2.1 *If F is weak positive dominant then $F \geq 0$ on $[0, 1]^n$. If f is positive dominant then $F > 0$ on $(0, 1]^n$.*

Proof: We prove Statement 1 first. Here is the 1 variable case. If $F(x)$ has degree 0 the result is clear. Given $x \in (0, 1]$ we have

$$F(x) = a_0 + \dots + a_n x^n \geq x((a_0 + a_1) + a_2 x + \dots + x^{n-1}).$$

The last polynomial is also weak positive dominant and satisfies the conclusion of the lemma by induction on the degree.

For the multivariable case, we write

$$F = f_0 + f_1 x_n + \dots + f_m x_n^m, \quad f_j \in \mathbf{R}[x_1, \dots, x_{n-1}]. \quad (9)$$

Let $F_j = f_0 + \dots + f_j$. Since F is weak positive dominant, F_j is weak positive dominant for all j . By induction on n , we get $F_j > 0$ on $[0, 1]^{n-1}$. But now, if we hold x_1, \dots, x_{n-1} fixed and let $t = x_n$ vary, the polynomial

$$g(t) = F(x_1, \dots, x_{n-1}, t)$$

is weak positive dominant.. Hence, by the 1 dimensional case, we get $g \geq 0$ on $[0, 1]$. Hence $F \geq 0$ on $[0, 1]^n$.

Now we prove Statement 2. If $\sum_{A_I} > 0$, we observe that for Ω sufficiently large and $\epsilon > 0$ sufficiently small, the modified polynomial

$$F^* = F - \epsilon(x_1 \dots x_n)^\Omega$$

is still weak positive dominant. Since $F^* \geq 0$ on $[0, 1]^n$, we have $F > 0$ on $(0, 1]^n$. ♠

Remark: The Positive Dominance criterion, and an associated recursive subdivision algorithm which uses it, is a powerful positivity certificate. I thought of this myself but I have always figured that it probably already exists somewhere in the computational algebra literature. I have never found a source, however.

3 Integrability

3.1 The Map in Coordinates

Every member $P \in \mathcal{P}_{8,2}$ has a canonical representative vertices

$$(1, 0), (a, b), (0, 1), (-d, c), (-1, 0), (-a, -b), (0, -1), (d, -c). \quad (10)$$

We label these vertices v_0, \dots, v_7 . We call $p = (a, b, c, d)$ the *coordinates* of P . When $(a, b) = (c, d)$ our point lies in the space $\mathcal{P}_{8,4}$ of 8-gons with 4-fold rotational symmetry.

When we apply the map T_3 we initially get a polygon P' with vertices v'_0, \dots, v'_7 , where

$$v'_k = \overline{v_{k+1}v_{k+4}} \cap \overline{v_{k+2}v_{k+5}},$$

where the indices are taken mod 8. One could use other labeling conventions, but this one leads to a nice formula for T_3 .

$$T_3 = A\Delta A\Delta,$$

Where

$$A(a, b, c, d) = (-b, -a, -d, -c), \quad (11)$$

and after setting $E = ac + bd$,

$$\Delta = \left(\frac{b(c+d+1)}{c(E+a+c+1)}, \frac{d(E+b+c)}{c(E+a+c+1)}, \frac{d(a+b+1)}{a(E+a+c+1)}, \frac{b(E+a+d)}{a(E+a+c+1)} \right) \quad (12)$$

The map Δ is especially nice because all its component functions are positive. Here are some symmetries of our map:

$$\begin{aligned} I(A\Delta)I &= A\Delta, & I(a, b, c, d) &= (c, d, a, b). \\ JT_3J &= IT_3, & J(a, b, c, d) &= (b, a, d, c). \end{aligned} \quad (13)$$

Since I commutes with $A\Delta$, we see that $IT_3I = T_3$. Also, J commutes with T_3^2 because

$$JT_3^2J = (JT_3J)(JT_3J) = (IT_3I)T_3 = T_3^2.$$

When it comes time to prove Theorem 1.2 we will use Equation 13 to reduce to the case when

$$a - b + c - d > 0. \quad (14)$$

The ‘‘square root map’’ $A\Delta$ behaves better with respect to these points.

3.2 Some Important Functions

Let \mathcal{I} denote the set of centrally symmetric 8-gons inscribed in a conic section. Let \mathcal{I}^* denote the set of centrally symmetric 8-gons circumscribed about a conic section. Define functions

$$g_{ab}^* = a-b, \quad g_{cd}^* = c-d, \quad g_{ab} = \frac{1-a^2-b^2}{ab}, \quad g_{cd} = \frac{1-c^2-d^2}{cd}. \quad (15)$$

A computation shows that

$$(a, b, c, d) \in \mathcal{I} \iff g_{ab} + g_{cd} = 0, \quad (a, b, c, d) \in \mathcal{I}^* \iff g_{ab}^* + g_{cd}^* = 0. \quad (16)$$

The first of these equations has a simple geometric interpretation. From the way we have normalized our 8-gons, the point (a, b) lies on the ellipse $x^2 + y^2 + g_{ab}xy = 0$. The point $(-c, d)$ lies on the ellipse $x^2 + y^2 - g_{cd}xy = 0$. If these points lie on the same ellipse then the constants are the same, meaning that $g_{ab} + g_{cd} = 0$. I don't know a nice geometric interpretation for the second equation, but it is an easy calculation.

The functions g_{ab} , etc., play a special role in the analysis of inscribed and circumscribed 8-gons. We deal with this in §9. They also serve as the building block for a T_3 -invariant function we call G . I discovered that the function

$$G(a, b, c, d) = 2(g_{ab} + g_{cd})(g_{ab}^* + g_{cd}^*) \quad (17)$$

is an invariant for T_3 . This is the most important invariant in the paper, the one we use the most.

After finding G , I looked for a second invariant. Referring to the literature on the pentagram map, say [15], I then guessed that the polynomial expression $(O_8/E_8)^{1/6}$ is an invariant for T_3 . The functions O_8 and E_8 are (now) called the *odd and even Casimirs* for the T_2 -invariant Poisson structure.

After finding these invariants, I played around with them until I came up with algebraically nicer ones, F_1 and F_2 , which satisfy the relations

$$F_2 - F_1 = G, \quad \frac{F_1}{F_2} = (O_8/E_8)^{1/6}. \quad (18)$$

In the next section I will describe F_1 and F_2 from scratch.

Remark: In spite of this discussion about the origins of F_1 and F_2 , the reader need not know anything about O_8 and E_8 to understand them.

3.3 The Integrability Proof

Let $e = ac + bd$. Our two basic invariants for T_3 are F_1 and F_2 where

$$\begin{aligned} F_1 &= \frac{(1+a-b)(1+c-d)(e+b-c)(e+d-a)}{abcd}, \\ F_2 &= \frac{(1-a+b)(1-c+d)(e-b+c)(e-d+a)}{abcd}. \end{aligned} \quad (19)$$

Referring to the maps in Equation 13, these functions obey the symmetries: $F_j \circ I = F_j$ and $F_{3-j} = F_j \circ J$. One can calculate in Mathematica directly that F_1 and F_2 are invariants for T_3 . By computing that ∇F_1 and ∇F_2 are linearly independent at some point, we see that F_1 and F_2 are algebraically independent.

The invariant symplectic form is.

$$\omega = \frac{1}{ab} \mathbf{d}a \wedge \mathbf{d}b + \frac{1}{cd} \mathbf{d}c \wedge \mathbf{d}d. \quad (20)$$

We will show that $\Delta_j^*(\omega) = -\omega$ for $j = 1, 2$. This implies that ω is T_3 invariant. Let Δ stand for one of $\{\Delta_1, \Delta_2\}$. Let Ψ denote the Jacobian of Δ , namely the 4×4 matrix of partial derivatives. Let v_i denote the i th variable from the list (a, b, c, d) . Thus $(v_1, v_2, v_3, v_4) = (a, b, c, d)$. Let $\epsilon_{ij} = 1$ when $(i, j) = (1, 2)$ or $(i, j) = (3, 4)$ and otherwise 0. Correspondingly, let e_1, e_2, e_3, e_4 be the standard basis vectors on \mathbf{R}^4 . Let $(a', b', c', d') = \Delta(a, b, c, d)$. The quantity $\Delta^*(\omega)(e_i, e_j)$ equals

$$\frac{1}{a'b'}(\Psi_{1i}\Psi_{2j} - \Psi_{2i}\Psi_{1j}) + \frac{1}{c'd'}(\Psi_{3i}\Psi_{4j} - \Psi_{4i}\Psi_{3j}) \stackrel{(1)}{=} \frac{-\epsilon_{ij}}{v_i v_j} = -\omega(e_i, e_j), \quad \forall i, j.$$

The equality with an exclamation point is a big Mathematica calculation that miraculously works out. The other equalities just come from the definition of how the pullback of a 2-form works.

Given the simple nature of ω we can write down the Hamiltonian vector field X_ϕ for a function $\phi : \mathbf{R}^4 \rightarrow \mathbf{R}$ in an explicit way. We have

$$X_\phi = (-ab\phi_b, ab\phi_a, -cd\phi_d, cd\phi_c). \quad (21)$$

Here $\phi_a = \partial\phi/\partial a$, etc. Note that even though ω has poles along the coordinate hyperplanes, the Hamiltonian vector field for a function is everywhere defined.

Let X_j be the Hamiltonian of F_j . Another Mathematica calculation shows that $\omega(X_1, X_2) = 0$. Now we have established all the points of Theorem 1.4. Here X_j is the Hamiltonian of F_j , as in the previous chapter.

3.4 Integral Curves

Let $X_G = X_2 - X_1$ be the Hamiltonian of $G = F_2 - F_1$. We let \mathcal{X} denote be the set of (a, b, c, d) such that all the factors of F_1, F_2, G are nonzero. For instance, $a, b, c, d \neq 0$ and $|a - b| < 1$ and $|c - d| < 1$ and $a - b + c - d \neq 0$.

Lemma 3.1 *The Hamiltonian X_G never vanishes on \mathcal{X} .*

Proof: Our proof is something of an overkill but it shows some beautiful and useful formulas. Recall that $G = 2(g_{ab}^* + g_{cd}^*)(g_{ab} + g_{cd})$. We also define $h = \log(ac/bd)$. We compute

$$X_G \cdot \nabla g_{ab}^* = 2(g_{ab}^* + g_{cd}^*)(1 - a + b)(1 + a - b)(a + b)/(ab). \quad (22)$$

$$X_G \cdot \nabla g_{cd}^* = 2(g_{ab}^* + g_{cd}^*)(1 - c + d)(1 + c - d)(c + d)/(cd). \quad (23)$$

$$X_G \cdot \nabla g_{ab} = -2(g_{ab} + g_{cd})(1 - a + b)(1 + a - b)(a + b)/(ab). \quad (24)$$

$$X_G \cdot \nabla g_{cd} = -2(g_{ab} + g_{cd})(1 - c + d)(1 + c - d)(c + d)/(cd). \quad (25)$$

$$X_G \cdot \nabla h = 2(g_{ab}^* + g_{cd}^*)((1 + a^2 + b^2)/(ab) + (1 + c^2 + d^2)/(cd)). \quad (26)$$

Equations 22 – 25 all vanish on \mathcal{X} only if $a + b = c + d = 0$. But then both ab and cd are negative. This makes Equation 26 nonzero. ♠

Say that a G -curve is a curve tangent to X_G everywhere. The above result says that \mathcal{X} is foliated by G -curves. Since one of the functions considered in Lemma 3.1 is strictly monotone along a given G -curve, we see that these curves exit every compact subset of \mathcal{X} at both ends.

3.5 A Special Dependent Set

There is a 2-dimensional T_3 -invariant set \mathcal{Y} consisting entirely of points where X_1 and X_2 are linearly dependent. The set \mathcal{Y} is given by equations that

$$ac + bd = -1, \quad ac^2 + ca^2 + bd^2 + db^2 = 0. \quad (27)$$

The invariants F_1 and F_2 are not constant on \mathcal{Y} and thus the T_3 orbits in \mathcal{Y} typically lie in 1-dimensional curves. On \mathcal{Y} , the invariants F_1 and F_2 satisfy $Y(F_1, F_2) = 0$ where

$$Y(F_1, F_2) = 512 + 216F_1F_2 + 192(F_1 + F_2) - 30(F_1 + F_2)^2 + (F_1 + F_2)^3. \quad (28)$$

Remark: I noticed that $p_a = (a, -a, -1/(2a), 1/(2a)) \in \mathcal{Y}$. I then computed

$$F_1(p_a) = g(a) := \frac{(1-a)(1-2a)(1-2a+2a^2)^2}{a^3}, \quad F_2(P_a) = g(-a).$$

I guessed that the curve $a \rightarrow (g(a), g(-a))$ would satisfy a symmetric integer polynomial equation and found the coefficients using linear algebra.

Lemma 3.2 *The invariants F_1 and F_2 are never both positive on \mathcal{Y} . Hence the level curve through a convex point is disjoint from \mathcal{Y} .*

Proof: A bit of calculus shows that $\nabla Y = 0$ only at the point $(-4, -4)$. Moreover $Y(u, 0) = (2+u)(16-u)^2$. From this formula and symmetry, $Y \geq 0$ on the boundary of the positive quadrant in the plane. Finally as $(u, v) \rightarrow \infty$ in the positive quadrant, we have $Y(u, v) \rightarrow +\infty$, because the cubic terms are all positive and they eventually dominate. From these properties we see that $Y > 0$ in the interior of the positive quadrant. The second statement follows from the fact that both F_1 and F_2 are both positive on convex points. ♠

3.6 Outline of the Proof

In this section we outline the proof of Theorem 1.2 for 8-gons which are neither inscribed nor circumscribed. We take care of the inscribed and circumscribed case in §9.

Step 1, Linear Independence: In §4 we prove that X_1 and X_2 are linearly dependent at all points of $\mathcal{X} - \mathcal{Y}$. The same therefore holds for the gradient ∇F_1 and ∇F_2 . Hence $\mathcal{X} - \mathcal{Y}$ is completely foliated by smooth and intrinsically flat surfaces.

Step 2, Cylindrical Components: Let \mathcal{X}_+ denote the component of \mathcal{X} where all the factors in F_1 and F_2 and G are positive. Thus, for instance, $(b-c) + ac + bd > 0$ and $a - b + c - d > 0$ and $|a - b| < 1$. Up to the action of the map J in Equation 13 all convex 8-gons which are neither inscribed nor circumscribed, nor 4-fold symmetric, are represented by points in \mathcal{X}_+ . Let L_+ be an arbitrary level set in \mathcal{X}_+ . In §5 we prove that L_+ is a finite union K of cylinders. Here K is independent of the choice of L_+ .

Step 3, The Nice Loop: Let \mathcal{U} denote the set (a, b, c, d) where $a, b, c, d > 0$ and $\max(a + b, c + d) = 1$. In §6 we prove that $K = 1$. That is, each level set L_+ in \mathcal{X}_+ is a single cylinder. The main step in the proof is showing that $L_+ \cap \mathcal{U}$ is a single piecewise smooth loop. We call this loop the *nice loop*. The nice loop is smooth away from two points satisfying $a + b = c + d = 1$.

Step 4, Intrinsic Boundedness and Concavity: In §7 we prove that each level set L_+ in \mathcal{X}_+ is bounded with respect to its intrinsic flat structure coming from its integrability. We also prove that L_+ is locally concave near its intrinsic boundary. We prove this by showing that the map $\iota_5 = A\Delta A\Delta A$ is an isometry of the sub-cylinder $L'_+ \subset L_+$ which lies to one side of the nice loop. This part of the proof is absolutely crucial: The map ι_5 swaps the boundary components of L'_+ and thus allows us to convert “internal information” about the nice loop into asymptotic information about a boundary component of L_+ . We also prove that $\Delta(L_+) = L_+$ and that Δ swaps the boundary components of ∂L_+ , so we can use the information about the one boundary component to get information about the other.

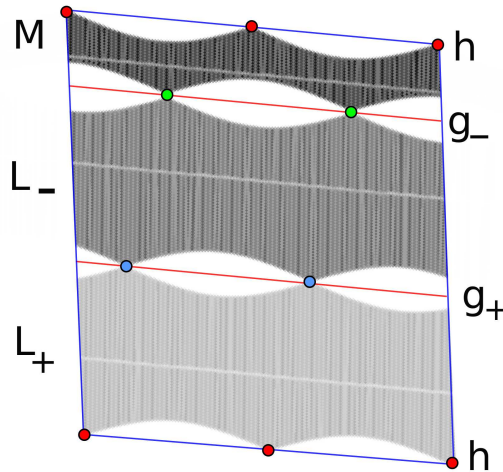


Figure 3: The intrinsic structure of $L(3, 4)$.

The bottom cylinder in Figure 3 is a numerical plot of L_+ , in its intrinsic flat structure, corresponding to the parameters $(F_1, F_2) = (3, 4)$. I drew this picture by numerically integrating linear combinations of X_1 and X_2 . The vertical foliation corresponds to $X_G = X_2 - X_1$. We call the points of non-concavity *cusps*. They correspond to the non-smooth points on the nice loop.

Step 5, Analytic Continuation: Let $L_- = A(L_+)$. Since A negates all the coordinates, $L_+ \cap L_- = \emptyset$. We show the existence of 2 intrinsically convex disks which serve as a mutual analytic continuation which “glues” L_+ and L_- together. The middle strip in Figure 3 shows L_- . We will see that there is one more cylinder M which touches L_+ and L_- at the cusps. There are 2 more convex disks which glue M to L_+ and 2 which glue M to L_- in the same sense as already discussed. All 6 disks are convex and isometric to each other. They are the white disks in Figure 3.

Let \widehat{L} denote the union of the cylinders L_+ , L_- , and M , together with the 6 convex disks mentioned. The space \widehat{L} is a flat torus. In Figure 3, the space $\widehat{L}(3, 4)$ is obtained by gluing opposite sides of the blue parallelogram together by translations. The geodesics labeled h and g_+ and g_- separate the open cylinders, because the intermediary disks are convex. In particular, L_+ is contained in the cylinder bounded by g_+ and h , and this cylinder has *less than half the height* of the whole torus.

As we will discuss more fully in §8, we have

$$A\Delta(h) = g_+, \quad T_3(h) = (A\Delta)^2(h) = g_-. \quad (29)$$

The first relation implies the second one. Since g_- and h are distinct, the vertical component of the translation induced by T_3 is nontrivial.

Step 6, Vertical Displacement: Suppose now that ξ represents a convex 8-gon which is neither inscribed nor circumscribed in an ellipse. In [16] we took care of the case when ξ has 4-fold symmetry. Thus, we can assume that ξ does not have 4-fold symmetry. We can also replace ξ by $J(\xi)$ to give us $\xi \in L_+$. Geometrically the 8-gons represented by ξ and $J(\xi)$ are obtained from each other by reflecting in the line $y = x$. Thus, if ξ represents a counter-example to Theorem 1.2 then by symmetry so does $J(\xi)$.

Since L_+ is contained in a strip of less than half the total height of \widehat{L} , and since the vertical component of the translation induced by T_3 is nontrivial, we see that the T_3 -orbit of any point in L_+ , including a convex point, eventually exits L_+ . But points outside L_+ are nonconvex.

The action of forward iterates of T_3 on ξ agrees with the translation action on the torus unless some power of T_3 is undefined. However, if $T_3^n(\xi)$ is convex for all n then all iterates are defined. But then there is some n such that $T_3^n(\xi) \notin L_+$ and the corresponding 8-gon is not convex.

4 The Independence Theorem

Let \mathcal{X} and \mathcal{Y} be the sets from the previous chapter. In this chapter we prove the following theorem.

Theorem 4.1 (Independence) *The Hamiltonians X_1 and X_2 are nonzero and linearly independent at each point of $\mathcal{X} - \mathcal{Y}$.*

4.1 Reduction to a Casy by Case Study

Throughout the proof, $N(\cdot)$ denotes the numerator function.

Using Equations 22 and 23 we see $X_G \cdot \mu = 0$, where

$$\mu = (\alpha, -\alpha, -\beta, \beta), \quad \alpha = \frac{4ab(c+d)}{(a-b+1)(-a+b+1)}, \quad \beta = \frac{4cd(a+b)}{(c-d+1)(-c+d+1)}$$

When the vectors X_1 and X_2 are linearly dependent we have $X_j \cdot \mu = 0$. To prove the Independence Theorem we consider polynomials

$$f_{uv} = N(\mathbf{d}u \wedge \mathbf{d}v(X_1, X_2)), \quad g = N(X_1 \cdot \mu). \quad (30)$$

Here $u, v \in \{a, b, c, d\}$. The denominators are monomials in a, b, c, d and so they do not vanish in \mathcal{X} . These polynomials all vanish when X_1 and X_2 are linearly dependent. For each $e \in \{a, b, c, d\}$ we define

$$h_e = \text{res}(f_{ab}, g, e). \quad (31)$$

Up to signs, we have

$$h_b(a, b, c, d) = h_a(b, a, d, c), \quad h_c(a, b, c, d) = h_a(c, d, a, b), \quad h_d(a, b, c, d) = h_a(d, c, b, a).$$

Thus we just need to give a formula for h_a . We have

$$\begin{aligned} h_a &= (-1+b)(1+b)(b-c)(b-d)(c+d)^2 \times \phi_1 \phi_2^2 \phi_3^2 \phi_4, \\ \phi_1(a, b, c, d) &= bc - c^2 + bd + cd \\ \phi_2(a, b, c, d) &= b - c + bc - c^2 - bd - cd \\ \phi_3(a, b, c, d) &= -b + c + bc - c^2 - bd - cd \\ \phi_4(a, b, c, d) &= 1 - c^2 + 2bd + b^2cd - bc^2d + b^2d^2 + bcd^2. \end{aligned}$$

If X_1 and X_2 are linearly dependent, then one factor from each expression h_a, h_b, h_c, h_d vanishes. We will go through the 9 factors for h_a and eliminate

all of them from consideration. If we have shown that the k th factor of h_a cannot vanish then by symmetry we have also shown this for each of h_b, h_c, h_d .

If X_1 and X_2 are linearly dependent at a point, then they are linearly dependent along the G -curve through this point, and multiples of X_G , because flow along X_G is a symplectomorphism. If some function ζ vanishes at a point of linear dependence, we can assume that $X_j \cdot \nabla \zeta = 0$ for $j = 1, 2$ and that $X_G \cdot \nabla \zeta = 0$. Otherwise we can make an arbitrarily small perturbation along the G -curve and produce a new point of linear dependence where $\zeta \neq 0$. We call this the *flow trick*.

4.2 Cases 1 and 2

If one of the first two factors of h_a vanishes, then we have $b = \pm 1$. The symmetry $(a, b, c, d) \rightarrow -(a, b, c, d)$ swaps these two cases. Thus, it suffices to consider the case that $b = 1$. By the flow trick,

$$X_1 \cdot (0, 1, 0, 0) = X_2 \cdot (0, 1, 0, 0) = 0.$$

Solving for a and c we find that the nonzero solutions are

1. $a = 1 + d$ and $c = -1$. In this case $F_2(1 + d, 1, -1, d) = 0$.
2. $a = -1$ and $c = 1 + d$. In this case $F_2(-1, 1, 1 + d, d) = 0$.
3. $a = 1 - (d^2/2)$ and $c = 1/(1 + d)$.

Only sub-case 3 gives points in \mathcal{X} . For these values, f_{ac} is a nontrivial polynomial in d . But then f_{ab} only vanishes at isolated points, a contradiction. This proves that $b \neq \pm 1$.

By symmetry, we eliminate the possibilities that $a, c, d \in \{-1, 1\}$.

4.3 Case 3

Suppose $b - c = 0$. By the flow trick,

$$X_G \cdot (0, 1, -1, 0) = -4(a - d)(a + d) = 0. \quad (32)$$

This forces $d = \pm a$. We have $G(a, b, b, \pm a) = 0$, so these point are not in \mathcal{X} . By symmetry we have also ruled out the possibility that $a - d = 0$.

4.4 Case 4

Suppose $b - d = 0$. By the flow trick we can assume that $b - d = 0$ along the flowline. We compute

$$0 = X_G \cdot (0, 1, 0, -1) = \frac{4(c - a)(a - b + c)(b^2 + ac - 1)}{ab}. \quad (33)$$

$$G(a, b, c, b) = \frac{2(a + c)(2b - a - c)(b^2 + ac - 1)}{abc} \quad (34)$$

If $c = a$ then we have $(a, b) = (c, d)$ and we are not in \mathcal{X} . If $b^2 + ac - 1 = 0$ we have $G(a, b, c, b) = 0$, by Equation 34. The only possibility is that $b = a + c$. We have

$$u_j = N(X_1 \cdot (0, 1, 0, -1)) = 0$$

along the flowline for $j = 1, 2$. Here u_1 and u_2 are polynomials in a and c . We compute that $\text{res}(u_1, u_2, a)$ and $\text{res}(u_1, u_2, c)$ are nontrivial. This is a contradiction.

By symmetry we have also eliminated the possibility that $a - c = 0$.

4.5 Case 5

Suppose $c + d = 0$. We first compute

$$g(a, b, c, -c) = c^4(1 - a + b)(1 + a - b)(a + b). \quad (35)$$

Since $|a - b| \neq 1$ we must have $a + b = 0$. We compute

$$0 = f_{ac} = -2ac(a - c)(1 + 2ac)(-a - c + 2ac)^2(a + c + 2ac)^2. \quad (36)$$

The solutions are:

1. $c = a$. Here $(a, b) = (c, d)$ and we are not in \mathcal{X} .
2. $c = (-a)/(2a \pm 1)$. Here $F_1 = 0$ or $F_2 = 0$, and we are not in \mathcal{X} .
3. $c = -1/(2a)$. In this case we are in \mathcal{Y} .

This eliminates the case $c + d = 0$. By symmetry we eliminate $a + b = 0$.

4.6 Case 6

Suppose $\phi_1 = 0$. This gives

$$b = \frac{c^2 - cd}{c + d}. \quad (37)$$

Note that we have already shown $c + d \neq 0$. By the flow trick,

$$0 = X_G \cdot \nabla \phi_1 = -\frac{4(ac + ad + cd - d^2)(2c + ac^2 + 2acd + c^2d + ad^2 - d^3)}{(c + d)^2}.$$

The two possibilities are:

$$a = \frac{-cd + d^2}{c + d}, \quad a = \frac{-2c - c^2d + d^3}{(c + d)^2}.$$

In the first case we have $a - b + c - d = 0$. This point does not lie in \mathcal{X} .

In the second case, f_{ab} and f_{ac} are rational functions in c, d . We check that both expressions

$$\text{res}(N(f_{ab}), N(f_{ac}), c), \quad \text{res}(N(f_{ab}), N(f_{ac}), d)$$

are nontrivial. So, we can have only isolated solutions to $\phi_1 = 0$, contradicting the fact that $\phi_1 = 0$ along the flowline.

4.7 Cases 7 and 8

The symmetry $(a, b, c, d) \rightarrow -(a, b, c, d)$ interchanges the two polynomials ϕ_2 and ϕ_3 . We suppose without loss of generality that $\phi_2 = 0$. This gives

$$b = \frac{c(1 + c + d)}{1 + c - d}. \quad (38)$$

Note that $|c - d| \neq 1$ and also $c + d + 1 \neq 0$ because $b \neq 0$.

Subcase 1: Suppose $c = -1/2$. By the flow trick

$$u_j = N(X_j \cdot (0, 0, 1, 0)) = 0$$

for $j = 1, 2$. These are polynomials in a and d and vanish along the flowline. But $\text{res}(u_1, u_2, a)$ and $\text{res}(u_1, u_2, d)$ are nontrivial. Hence u_1, u_2 cannot vanish along the flowline, a contradiction.

Subcase 2: The same argument shows that $a - c^2 - 1 \neq 0$.

Subcase 3: Suppose that $\zeta = a + ac - d - ad + cd + d^2 = 0$. When we expand out $F_2(a, b, c, d)$ with b as in Equation 38 we see that ζ is one of the factors. So, if $\zeta(a, b, c, d) = 0$ then $F_2(a, b, c, d) = 0$. Contradiction.

General Case: By the flow trick,

$$X_2 \cdot \nabla \phi_2 = \frac{\zeta^2(1+c)}{a(1+c-d)(1+c+d)} \times \mu_1 = 0. \quad (39)$$

Here μ_1 is some irreducible polynomial. The denominator does not vanish, and $c \neq 1$ and $\zeta \neq 0$. Hence $\mu_1 = 0$ along the flowline. We compute

$$\text{res}(\mu_1, N(f_{ab}), d) = 2^{22} a^5 c^6 (a-1)^2 (c-1)^2 (c+1)^{12} (1+2c)^2 (a-c^2-1)^2 \mu_2, \quad (40)$$

$$\text{res}(N(f_{ab}), N(f_{ac}), d) = 2^{15} a^3 c^4 (a-1)^2 (c-1)^2 (c+1)^{14} (a-c^2-1) \mu_3, \quad (41)$$

Here μ_2 and μ_3 are irreducible polynomials in a and c . Given the special cases above, we have $\mu_2 = \mu_3 = 0$ along the flowline. Finally, we compute that $\text{res}(\mu_2, \mu_3, a)$ and $\text{res}(\mu_2, \mu_3, c)$ are both nontrivial, a contradiction.

4.8 Case 9

The only possibility left is that

$$\phi_4(a, b, c, d) = \phi_4(b, a, d, c) = \phi_4(c, d, a, b) = \phi_4(d, c, b, a) = 0.$$

If $bd + 1 = 0$ then

$$\phi_4(a, b, c, d) = \frac{c(1-d)(1+d)}{d} = 0 \quad \implies \quad d = \pm 1.$$

We have already ruled this out. Hence $bd + 1 \neq 0$. Solving $\phi_4(a, b, c, d) = 0$ for a and c we find that a and c are roots of the same quadratic polynomial

$$Ax^2 + Bx + C = 0, \quad A = -1 - bd, \quad B = bd(b+d), \quad C = (1+bd)^2. \quad (42)$$

By Case 3 and symmetry, we have $a \neq c$. Hence a and c must be distinct roots. The quadratic formula gives

$$a + c = \frac{-B}{A} = \frac{bd(b+d)}{1+bd}. \quad (43)$$

Rearranging this and clearing the nonzero demoninator, we find that

$$-a - c - abd - bcd + b^2d + bd^2 = 0. \quad (44)$$

Playing the same game with (b, d) in place of (a, c) we see that

$$-b - d - cda - dab + c^2a + ca^2 = 0 \quad (45)$$

Subtracting Equation 44 from Equation 45 we get

$$(a - b + c - d)(ac + bd + 1) = 0. \quad (46)$$

The first of these factors does not vanish in \mathcal{X} . Hence $ac + bd = 1$. This is one of the defining equations for \mathcal{Y} . Adding Equations 44 and 45 we get

$$-(a + b + c + d) + (ca^2 + ac^2 + bd^2 + db^2) - (abc + abd + acd + bcd) = 0. \quad (47)$$

Finally, we use $ac + bd = 1$ to convert Equation 47 to the simpler relation

$$ac^2 + ca^2 + bd^2 + db^2 = 0,$$

the other defining equation for \mathcal{Y} .

This computes the proof of the Independence Theorem.

5 Cylinders in the Positive Part

5.1 The Main Result

Recall that \mathcal{X}_+ is the subset of \mathcal{X} where every factor of F_1, F_2, G is positive. In this chapter we prove the following result.

Theorem 5.1 *Each level set L_+ in \mathcal{X}_+ is bounded in \mathbf{R}^4 , and also a finite union of K cylinders. Here K does not depend on the level set.*

Here is an outline of the proof. Recall that a G -curve of L_+ is one that is integral to X_G . We consider G -curves to be subsets of \mathcal{X}_+ .

1. We prove the L_+ is bounded in \mathbf{R}^4 .
2. Let \mathcal{T} denote the hyperplane $a + c = 2$. By analyzing the ends of G -curves and also by making an explicit calculation, we see that each G -curve of L_+ intersects \mathcal{T} transversely and precisely once.
3. We prove that all components of $L_+ \cap \mathcal{T}$ are closed loops.
4. The steps above imply that L_+ is foliated by G -curves which intersect \mathcal{T} transversely and precisely once. Hence L_+ is a finite union of K cylinders. The number K also counts the number of loops in $L_+ \cap \mathcal{T}$.
5. We show that \mathcal{X}_+ is connected. By continuity and transversality, K is locally constant. Since \mathcal{X}_+ is connected, K is constant.

5.2 Bounded Level Sets

Lemma 5.2 *The level set L_+ is bounded in \mathbf{R}^4 .*

Proof: We work with the functions g_{ab} and g_{cd} from Equation 15. (We repeat the formula for g_{ab} on the next page.) Suppose $\{(a_n, b_n, c_n, d_n)\}$ is an unbounded sequence in L_+ . By symmetry it suffices to consider the case when one of c_n or d_n tends to ∞ . Since $|c_n - d_n| < 1$, both of these coordinates tend to ∞ . Hence $g_{cd}(a_n, b_n, c_n, d_n) \rightarrow -2$. We will show that $g_{ab}(c_n, b_n, c_n, d_n) \rightarrow +2$. Since $g_{ab}^*, g_{cd}^* \in (0, 2)$ we get $G(a_n, b_n, c_n, d_n) \rightarrow 0$, a contradiction. This function is nonzero and constant along L_+ .

Case 1: Suppose that $a_n + b_n \geq 1$ for all n . An exercise in Lagrange multipliers tells us that in this case that $g_{ab} < 2$ in this case. Since $g_{ab} + g_{cd} > 0$ and $g_{cd} \rightarrow -2$ we must have $g_{ab} \rightarrow 2$. This gives us our contradiction.

Case 2: Suppose $a_n + b_n < 1$ and a_n and b_n both remain in a compact subset of the interval $(0, 1)$. We have

$$a_n - d_n + a_n c_n + b_n d_n > 0 \quad (48)$$

because this expression is a factor of F_2 . Since $c_n/d_n \rightarrow 1$ and both terms go to $+\infty$, we must have $a_n + b_n \rightarrow 1$. If a_n and b_n remain in a compact subset of the open interval $(0, 1)$ then again $g_{ab}(a_n, b_n, c_n, d_n) \rightarrow 2$. This gives us the same contradiction as in Case 1.

Case 3: After passing to a subsequence, it only remains to consider what happens when $a_n + b_n < 1$ and $(a_n, b_n) \rightarrow (1, 0)$ or $(a_n, b_n) \rightarrow (0, 1)$. We treat the second case; the first then follows from symmetry.

Let us examine Equation 48 again. Because $c_n < d_n + 1$ we get

$$0 < a_n - d_n + a_n c_n + b_n d_n < a_n + a_n(d_n + 1) - d_n + b_n d_n = (a_n + b_n - 1)(d_n) + 2a_n.$$

Rearranging the last inequality, we have

$$\frac{1 - b_n}{a_n} < 1 + \epsilon, \quad \epsilon = \frac{2}{d_n}.$$

Since $d_n \rightarrow \infty$ we can take $\epsilon > 0$ as small as we like. But then

$$\frac{1 - a_n^2 - b_n^2}{a_n} < \frac{1 - b_n^2}{a_n} = (1 + b_n) \times \frac{1 - b_n}{a_n} < 2 + 2\epsilon.$$

Since $b_n \rightarrow 1$ we have

$$g_{ab}(a_n, b_n, c_n, d_n) = \frac{1 - a_n^2 - b_n^2}{2a_n b_n} < 2 + 2\epsilon \quad (49)$$

once n is sufficiently large. Since ϵ is arbitrary, we see that $g_{ab} \rightarrow 2$ and we get the same contradiction. ♠

5.3 The Ends of Integral Curves

In this section we consider an integral G -curve contained in the level set L_+ . We start with a result that does not mention G -curves.

Lemma 5.3 *Any accumulation point of L_+ that does not lie in \mathcal{X} has the following form.*

1. $(\bar{a}, 0, 0, \bar{a})$ for $\bar{a} \in [0, 1)$ or $(0, \bar{b}, \bar{b}, 0)$ for $\bar{b} \in [0, 1)$.
2. $(1, 0, \bar{c}, \bar{d})$ for $\bar{c} + \bar{d} \geq 1$ or $(0, 1, \bar{c}, \bar{d})$ for $\bar{c} + \bar{d} \geq 1$.
3. $(\bar{a}, \bar{b}, 1, 0)$ for $\bar{a} + \bar{b} \geq 1$ or $(\bar{a}, \bar{b}, 0, 1)$ for $\bar{a} + \bar{b} \geq 1$.

Proof: The denominators of each invariant F_1, F_2, G are of the form $abcd$ and moreover these invariants are constant along L_+ . Hence every accumulation point $(\bar{a}, \bar{b}, \bar{c}, \bar{d})$ of L_+ outside of \mathcal{X} must have at least one zero coordinate. We suppose that either $\bar{a} = 0$ or $\bar{b} = 0$. The other cases follow from symmetry.

Case 1: Let g_{ab} and g_{cd} be as in Equation 15. Suppose first that $\bar{a} = 0$ and $\bar{b} < 1$. Then $g_{ab} \rightarrow +\infty$. Also, $g_{cd} > -1$. This latter inequality is a rearrangement of the inequality $(c-d)^2 < 1$. We conclude that $a-b+c-d \rightarrow 0$. Hence our point is $(0, \bar{b}, \bar{b} + t, t)$ for some $t \geq 0$, and

$$F_1(a, b, c, d) = \frac{(1+a-b)(1+c-d)(b-c+ac+bd)(d-a+ac+bd)}{abcd}.$$

Since the denominator tends to 0 as we accumulate on our point, so must the numerator. The numerator converges to

$$(1 - \bar{b})^2(-t + \bar{b}t)(+t + \bar{b}t). \quad (50)$$

Since $\bar{b} < 1$ this forces $t = 0$. Hence, our accumulation point is $(0, \bar{b}, \bar{b}, 0)$. The same argument works when $\bar{a} < 1$ and $\bar{b} = 0$.

Case 2: Suppose that $\bar{a} = 0$ and $\bar{b} \geq 1$. Since $|a - b| < 1$ along L_+ we must have $\bar{b} = 1$. Since $c - b + ac + bd > 0$ along L_+ , we have

$$\bar{c} - 1 + \bar{d} = \bar{c} - \bar{b} + (0)(\bar{c}) + (1)\bar{d} \geq 0.$$

In short $\bar{c} + \bar{d} \geq 1$. The case when $\bar{b} = 0$ and $\bar{a} = 1$ has the same treatment. ♠

From the discussion following Lemma 3.1, each G -curve χ exits every compact subset of \mathcal{X}_+ at both ends. Since L_+ is bounded, each end of χ accumulates on at least one point of \mathbf{R}^4 .

Lemma 5.4 *The backwards end of any G -curve has a unique accumulation point, and it has the form $(x, 0, 0, x)$ or $(0, x, x, 0)$ for some $x \in [0, 1)$. The forwards end of any G -curve has a unique accumulation point, and it has the form $(1, 0, x, y)$ or $(x, y, 1, 0)$ for some (x, y) with $x > 0$ and $x + y \geq 1$.*

Proof: Suppose the backwards end of χ accumulates on $(1, 0, 0, 1)$. By Equation 22, the quantity $a - b$ increases along χ but remains less than 1. This is an immediate contradiction. The same argument, using one of Equation 22 or 23, rules out $(0, 1, 1, 0)$ and $(1, 0, x, y)$ and $(x, y, 1, 0)$ as backwards accumulation points. Suppose $(0, 1, x, y)$ is a backwards accumulation point. Since $a - b + c - d > 0$ in \mathcal{X}_+ we must have $x - y \geq 1$. But, again, this contradicts the fact that $c - d$ increases along χ and always satisfies $c - d < 1$. The same argument rules out $(x, y, 0, 1)$ as a limit point. Lemma 5.3 now says that any accumulation point has the claimed form.

The uniqueness of the backwards accumulation point follows from the characterization of the backwards accumulation points and from the monotonicity of g_{ab}^* and g_{cd}^* .

Suppose that the forward end of χ accumulates on $(a', 0, 0, a')$. This contradicts the monotonicity of $a - b$ and $c - d$ along χ and the form of the backwards limit point. The same argument rules out $(0, b', b', 0)$. If $(0, 1, x, y)$ is a forward accumulation point, then by monotonicity we would have $a - b < -1$ along χ . This is a contradiction. The same argument rules out $(x, y, 0, 1)$. Arguments like we have already given rule out $(0, 1, 1, 0)$ and $(1, 0, 0, 1)$. Lemma 5.3 now says that any accumulation point has the claimed form.

The uniqueness is more subtle here. If the uniqueness is false, then really we have a whole continuum of accumulation points. By continuity and symmetry we can find a single G -curve having accumulation points $(1, 0, x_1, y_1)$ and $(1, 0, x_2, y_2)$ with $x_1, y_1, x_2, y_2 > 0$. But then the monotonicity implied by Equations 23 and 25 says that g_{cd} and g_{cd}^* both are finite and coincide on these points. This forces the points to coincide. ♠

5.4 The Median Surface

Let \mathcal{T} be the surface given by $a + c = 1$.

Lemma 5.5 $X_G \cdot (1, 0, 1, 0) > 0$ everywhere in $\mathcal{T} \cap \mathcal{X}$. Hence each G -curve in the level set L_+ intersects \mathcal{T} transversely, and only once.

Proof: By Lemma 5.4, each G -curve in L_+ does indeed intersect \mathcal{T} because $a + b < 1$ near the backwards end and $a + c > 1$ near the forwards end.

We let $c = 1 - a$ and we consider the polynomial

$$\phi_1(a, b, d) = \frac{2}{abcd} X_G \cdot (1, 0, 1, 0).$$

It suffices to prove that $\phi_1 > 0$ whenever $a \in (0, 1)$ and $b, d \in (0, 1)$ and $b + d \in (0, 1)$. To use our positivity certificate we change variables. Let

$$\phi_2(a, u, v) = \phi_1(a, 1 - u, uv). \quad (51)$$

The domain $(a, u, v) \in (0, 1)^3$ corresponds to our domain above. We have

$$\begin{aligned} \phi_2 = & 2a^3 - a^4 + 2a^2u - 7a^3u + 3a^4u - 2a^2u^2 + 5a^3u^2 - 2a^4u^2 \\ & - a^3uv + a^4uv + 4au^2v - 4a^2u^2v - 5au^3v + 5a^2u^3v + 2au^4v - \\ & 2a^2u^4v - 2au^2v^2 + 3a^3u^2v^2 - 2a^4u^2v^2 + 2u^3v^2 - au^3v^2 + \\ & a^2u^3v^2 - u^4v^2 - 2au^3v^3 + 2a^2u^3v^3 + 2au^4v^3 - 2a^2u^4v^3. \end{aligned}$$

The polynomial $\phi(a, u, v)$ is not positive dominant, but subdivision helps. Let $I = (0, 1/2]$ and $J = (1/2, 1]$. A calculation shows that the following 4 polynomials are positive dominant

$$\phi_2\left(\frac{a}{2}, \frac{u}{2}, v\right), \quad \phi_2\left(\frac{a}{2}, 1 - \frac{u}{2}, v\right), \quad \phi_2\left(1 - \frac{a}{2}, \frac{u}{2}, v\right), \quad \phi_2\left(1 - \frac{a}{2}, 1 - \frac{u}{2}, v\right)$$

These results shows respectively that ϕ is positive on the domains

$$I \times I \times (0, 1], \quad I \times J \times (0, 1], \quad J \times I \times (0, 1], \quad J \times J \times (0, 1].$$

In particular, $\phi_2 > 0$ on $(0, 1)^3$. But then $\phi_1 > 0$ on the (a, b, d) -domain mentioned above. ♠

Let L_+ be a level set in \mathcal{X}_+ . By the previous result, L_+ is everywhere transverse to \mathcal{T} . Hence $L_+ \cap \mathcal{T}$ is a smooth 1-manifold.

Lemma 5.6 $L_+ \cap \mathcal{T}$ consists of a finite union of closed loops.

Proof: If this is false then we can find a sequence of points in $L_+ \cap \mathcal{T}$ which converge to a point of $\partial\mathcal{X}$. The limit point must be of the kind from Lemma 5.3. At the same time, points in $L_+ \cap \mathcal{T}$ satisfy

$$b + d < a + c = 1, \quad |a - b|, |c - d| < 1.$$

From these constraints, and from the list in Lemma 5.3, we see that the only possible limit points are $(1, 0, 0, 1)$ or $(0, 1, 1, 0)$. By symmetry, it suffices to rule out the possibility of $(1, 0, 0, 1)$.

We suppose this is false and derive a contradiction. We analyze the situation for a point $(a, b, c, d) \in L \cap \mathcal{T}$ near $(1, 0, 0, 1)$. To see the asymptotics, we set

$$a = 1 - \alpha, \quad b = \beta, \quad c = \alpha, \quad d = 1 - \beta - \gamma.$$

In this situation $\alpha, \beta, \gamma > 0$ and we want to consider the case when these numbers are small. We compute the $F_1(a, b, c, d)$ equals

$$\frac{(2 - \alpha - \beta)(2\beta - \alpha^2 - \beta^2 - \beta\gamma)(2\alpha - \alpha^2 - \beta^2 - \beta\gamma - \gamma)(\alpha + \beta + \gamma)}{\alpha\beta(1 - \alpha)(1 - \beta - \gamma)}. \quad (52)$$

In writing this expression we have been careful to factor in Mathematica in such a way that the signs are preserved. The third and fourth factors in the numerator of $F_1(a, b, c, d)$ are

$$(b - c) + ac + bd = 2\beta - \alpha^2 - \beta^2 - \beta\gamma < 2\beta,$$

$$(d - a) + ac + bd = 2\alpha - \alpha^2 - \beta^2 - \beta\gamma - \gamma > 2\alpha.$$

The significant thing is that 2α and 2β respectively are the only positive terms in these expressions and moreover these expressions are both positive by definition of \mathcal{X}_+ . Therefore, once $\alpha + \beta + \gamma < 1/2$ we have

$$F_1(a, b, c, d) < \frac{(1)(2\beta)(2\alpha)(\alpha + \beta + \gamma)}{\alpha\beta(\frac{1}{2})(\frac{1}{2})} \leq 16(\alpha + \beta + \gamma).$$

But this means that $F_1(a, b, c, d) \rightarrow 0$ as $(a, b, c, d) \rightarrow (1, 0, 0, 1)$ inside $L_+ \cap \mathcal{T}$. This is a contradiction. ♠

Corollary 5.7 $(1, 0, 0, 1)$ and $(0, 1, 1, 0)$ are not accumulation points of L_+ .

Proof: We consider $p = (1, 0, 0, 1)$. The case of $(0, 1, 1, 0)$ is similar. Suppose there is a sequence $\{p_n\} \in L$ converging to p . We write $p_n = (a_n, b_n, c_n, d_n)$. There is a sequence $\{\chi_n\}$ of G -curves in L_+ such that $p_n \in \chi_n$. Let $p'_n = (a'_n, b'_n, c'_n, d'_n) \in \mathcal{T}$ be the intersection of χ_n with \mathcal{T} . Since $L \cap \mathcal{T}$ is compact, we can pass to a subsequence so that $p \rightarrow p' = (a', b', c', d') \in L \cap \mathcal{T}$. Since $a_n - b_n \rightarrow 1$, and $a'_n - b'_n < 1$, and $a - b$ increases along χ we see that $a'_n - b'_n \rightarrow 1$. Hence $a' - b' = 1$. This contradicts the fact that $p' \in \mathcal{X}_+$. ♠

Corollary 5.8 The space \mathcal{X}_+ is path connected.

Proof: Since every G -curve of every level set in \mathcal{X}_+ intersects \mathcal{T} . It suffices to prove that $\mathcal{X}_+ \cap \mathcal{T}$ is connected. We use the same parametrization as in Equation 52. The positivity of all the factors of F_1 gives us the constraints

$$\alpha + \beta + \gamma < 1, \quad \alpha^2 + \beta^2 + \beta\gamma < 2\beta, \quad \alpha^2 + \beta^2 + \beta\gamma + \gamma < 2\alpha. \quad (53)$$

The positivity of all the factors of F_2 gives us the constraints

$$\alpha + \beta + \gamma < 1, \quad \alpha^2 + \beta^2 + \beta\gamma - \gamma < 2\beta, \quad \alpha^2 + \beta^2 + \beta\gamma < 2\alpha.$$

The constraints $|a - b| < 1$ and $|c - d| < 1$ give rise respectively to $\alpha + \beta < 1$ and $\alpha + \beta + \gamma < 1$. All these additional constraints are subsumed by Equation 53. Therefore $\mathcal{X}_+ \cap \mathcal{T}$ is diffeomorphic to the set Σ of all positive (α, β, γ) satisfying Equation 53.

If $(\alpha, \beta, \gamma) \in \Sigma$ and $\alpha > \beta$ we consider the curve

$$t \rightarrow (t^{3/2}\alpha, t\beta, t^2\gamma), \quad t \in (0, 1).$$

The first constraint is obviously satisfied by the points along this curve. For the other two constraints, the left hand side is multiplied by a factor no larger than t^2 and the right hand side is multiplied by a factor no smaller than $t^{3/2}$. We conclude that all points along our curve satisfy Equation 53. Thus, we can connect our point (α, β, γ) to a point of the form (δ, δ, γ) with $\gamma < \delta < 1/3$ by a path in Σ . A similar trick works when $\beta > \alpha$.

The constraint on the point (δ, δ, γ) is just $2\delta^2 + \delta\gamma + \gamma < 2\delta$. Hence we can increase γ until $\gamma = \delta$ and remain in Σ . Thus, we can connect any point in Σ to the set $(0, 1/3)^3 \subset \Sigma$ by a path in Σ . Hence Σ is connected. ♠

6 The Nice Loop

6.1 Overview

Let $L_+(f_1, f_2)$ is the level set in \mathcal{X}_+ corresponding to $F_1 = f_1$ and $F_2 = f_2$. Let \mathcal{U} be as in Step 4 of our outline in §3.6. We prove the following when $t > 0$ is sufficiently small.

1. Every connected component Σ of $L_+(4 - t, 4)$ intersects \mathcal{U} .
2. $L_+(4 - t, 4) \cap \mathcal{U}$ is a single loop.

From these two items we see that $K = 1$ in Theorem 5.1. We prove more generally that $L_+ \cap \mathcal{U}$ is always a single loop. This is our nice loop from Step 4 of our outline in §3.6.

6.2 Transversality

In this section we begin the study of $L_+ \cap \mathcal{U}$. We write

$$\mathcal{U} = \mathcal{U}_{ab} \cup \mathcal{U}_{cd} \tag{54}$$

where \mathcal{U}_{ab} is the set of points (a, b, c, d) where $a + b = 1$ and $c + d \leq 1$, and \mathcal{U}_{cd} has the same description but with (a, b) swapped with (c, d) .

Lemma 6.1 *L_+ is transverse to \mathcal{U}_{ab} and to \mathcal{U}_{cd} . Moreover each G -curve in L_+ intersects \mathcal{U} at most once.*

Proof: By symmetry it suffices to consider \mathcal{U}_{ab} . Since L_+ is smooth it suffices to prove that X_G is not tangent to \mathcal{U}_{ab} . The vector $(1, 1, 0, 0)$ is perpendicular to this space, and

$$X_G \cdot (1, 1, 0, 0) = \frac{4a(1 - a)(1 + c - d)(1 - c + d)}{cd} \neq 0. \tag{55}$$

This does it. Here we have used $b = 1 - a$ to simplify the expression.

The forward direction of a G -curve has a positive dot product with the normal to \mathcal{U} whenever it hits. But then it cannot come back and hit a second time because it would be returning in such a way as to make negative dot product with the same vector. For intersections which lie in $\mathcal{U}_{ab} \cap \mathcal{U}_{cd}$ we can use either $(1, 1, 0, 0)$ or $(0, 0, 1, 1)$ for this argument. ♠

6.3 Existence of a Nice Loop

We say that a *nice loop* in \mathcal{U} is one which intersects $\mathcal{U}_{ab} \cap \mathcal{U}_{cd}$ exactly twice and is preserved by the map $(a, b, c, d) \rightarrow (c, d, a, b)$. (Later on we will see that this loop is unique.) In this section we prove

Lemma 6.2 $L_+ \cap \mathcal{U}$ contains a nice loop for all level sets L_+ in \mathcal{X}_+ .

It is convenient to work with the invariants

$$G = F_2 - F_1, \quad H = F_1/F_2. \quad (56)$$

We concentrate on $L_+ \cap \mathcal{U}_{ab}$. Thus, we are interested in points $(a, 1 - a, c, d)$ with $c, d > 0$ and $c + d < 1$. This is a triangle τ in the (c, d) -plane. It is yellow in Figure 4 below.

Solving the equation $H(a, 1 - a, c, d) = h$, we find that

$$a = \frac{2d + h - ch - dh}{1 - c + d + h + ch - dh}. \quad (57)$$

Let us check that this equation is valid on τ . Setting $a = 0, 1, \infty$ respectively, we find that

$$h = \frac{2h}{c + d - 1} < 0, \quad h = \frac{c + d - 1}{2c} < 0, \quad h = \frac{-1 + c - d}{1 + c - d} < 0.$$

But $h > 0$. So, whenever (c, d) are in τ , the formula gives $a \in (0, 1)$ and it does not blow up. We write

$$\Gamma = G(a(c, d), 1 - a(c, d), c, d) - g = \frac{N}{D}, \quad (58)$$

$$D = cd(1 - c + d + h + ch - dh)$$

$$\begin{aligned} N = & 2 - 4c + 4c^3 - 2c^4 - 4d - 4c^2d + 8c^3d - 4cd^2 - 12c^2d^2 + 4d^3 + 8cd^3 - \\ & 2d^4 + cdg - c^2dg + cd^2g - 2h + 4ch - 4c^3h + 2c^4h + 4dh + 4c^2dh - \\ & 8c^3dh + 4cd^2h + 12c^2d^2h - 4d^3h - 8cd^3h + 2d^4h + cdgh + c^2dgh - cd^2gh \end{aligned}$$

Setting $D = 0$ and solving for h we find that $h = \frac{(-1+c-d)}{(1+c+d)} < 0$. Hence $G = g$ on τ iff $N = 0$. The intersections of $L_+ \cap \mathcal{U}_{ab}$ correspond to points (c, d) where $N(c, d) = 0$. We let V_N be this set.

Example: Figure 4 shows a contour plot of N for $g = 1$ and $h = 3/4$. This case corresponds to $(F_1, F_2) = (3, 4)$.

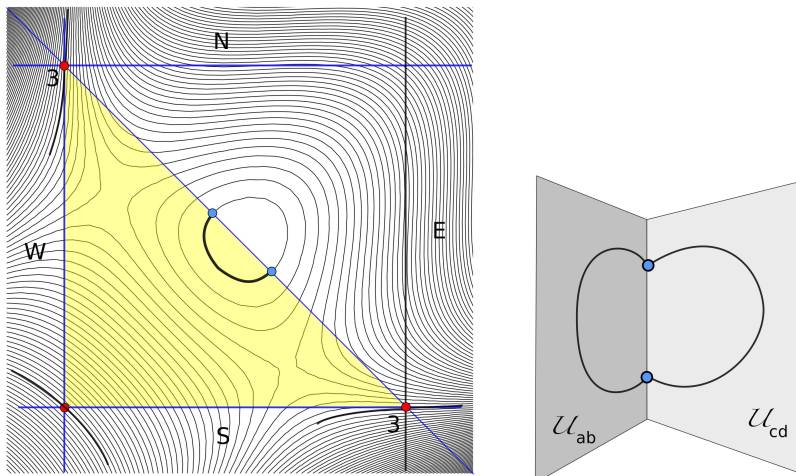


Figure 4: A contour plot (left) and a schematic picture (right).

In Figure 4 (left), the open yellow region τ is the region of interest to us. The set $\Gamma = 0$ has 4 planar components. The portion of the component in τ is exactly $L_+ \cap \mathcal{U}_{ab}$. The boundary points of this arc are swapped by the map $(a, b, c, d) \rightarrow (c, d, a, b)$ and together the two arcs $L_+(3, 4) \cap \mathcal{U}_{ab}$ and arcs $L_+(3, 4) \cap \mathcal{U}_{cd}$ join together at these points to make a nice embedded loop which is precisely $L_+(3, 4) \cap \mathcal{U}$. Figure 4 (right) shows this schematically. Note that the right half of this schematic picture is not the continuation of the level set from Figure 4 (left).

Here are some observations about N which hold for all $g > 0$ and all $h \in (0, 1)$ which correspond to level sets in \mathcal{X}_+ . It is important to remark that we only look at pairs (g, h) corresponding to such level sets.

1. Γ is quartic in c and d . Hence any straight line intersects V_N at most 4 times by Bezout's Theorem.
2. We compute that $\Gamma(0, d) = 2(1 - h)(d - 1)^3(d + 1)$. From this we see that the line $c = 0$ intersects V_N a total of 4 times counting multiplicity. The point $(0, 1)$ is a point of multiplicity 3 and the point $(0, -1)$ is a point of multiplicity 1. This is why we have added the number 3 in several places in Figure 4.

3. For at least one parameter choice, say the one in the plot, the level set through $(0, 1)$ goes from region N to region W , bypassing τ entirely. This cannot change because then at some parameter we would have an inflection point corresponding to multiplicity 4.
4. The level set through $(-1, 0)$ goes from S to W , completely bypassing τ . One can see this for a single parameter in a plot and then the same multiplicity argument shows that it is always true.
5. Similar statements holds for the line $d = 0$.

Using continuity, transversality, and the observations above, we see that $\partial\tau$ is a barrier for any component of V_N that starts in τ . The component is trapped in τ . To finish our claim about the existence of a nice loop, we just have that V_N always intersects the line $c + d = 1$ at 2 distinct points on the open segment σ bounded by $(1, 0)$ and $(0, 1)$. Once we know this, the two strants of V_N emanating from these points have no choice to connect to each other and make an arc. There is nowhere else for them to go.

Lemma 6.3 *V_N always intersects the line $c + d = 1$ at 2 distinct points on the open segment σ bounded by $(1, 0)$ and $(0, 1)$.*

Proof: By Bezout's Theorem, there can be at most 2 intersections, because the line extending σ contains $(1, 0)$ and $(0, 1)$. Plugging in a single choice of (g, h) , say the ones for the plot, we see that there are 2 intersection points. What could go wrong as we vary the level set continuously? If the two intersection points coalesce into 1 point $(a, 1 - c, c, 1 - c)$ then the map

$$(a, b, c, d) \rightarrow (c, d, a, b)$$

fixed this point. This forces $c = a$. But such points belong to level sets in $\mathcal{P}_{8,4}$. This is a contradiction.

The only thing we need to rule out is the possibility that our two intersection points move into the boundary. We compute

$$\Gamma(c, 1 - c) = -2c(1 - c)\Gamma_0(c),$$

$$\Gamma_0(c) = 16c - 16c^2 - g + cg - 16ch + 16c^2h - cgh.$$

The factor $2c(1 - c)$ accounts for the roots at $(1, 0)$ and $(0, 1)$. We compute $\Gamma_0(0) = -g$ and $\Gamma_0(1) = -gh$. These quantities do not vanish, so the intersection points cannot move into the boundary. ♠

6.4 Uniqueness of the Nice Loop

Recall that \mathcal{T} is the set given by $a + c = 1$. This is the set we considered at length in the previous chapter.

Lemma 6.4 *For any $\epsilon > 0$ there is some sufficiently small $t > 0$ such that $L_+(4 - t, 4) \cap \mathcal{T}$ lies within ϵ of the point $(1/2, 1/2, 1/2, 1/2)$.*

Proof: An exercise in calculus shows that $\phi(a, b) = F_1(a, b, 1 - a, 1 - b)$ has a unique global maximum on the domain $(0, 1)^2$. The value of the maximum is 4 and the location is $(a, b) = (1/2, 1/2)$.

Consider a point $(a_t, b_t, c_t, d_t) \in L \cap \mathcal{T}$. As $t \rightarrow 0$ we have

$$G(a_t, b_t, c_t, d_t) \rightarrow 0$$

regardless of the point choice. But then one of the two quantities

$$a_t - b_t + c_t - d_t, \quad \frac{1 - a_t^2 - b_t^2}{a_t b_t} + \frac{1 - c_t^2 - d_t^2}{c_t d_t}$$

tends to 0. Since $a_t + b_t = 1$ and $c_t + d_t < 1$ the latter expressions at least 2. Hence $a_t - b_t + c_t - d_t \rightarrow 0$ as $t \rightarrow 0$. Since $a_t + c_t = 1$ we have $b_t + d_t \rightarrow 1$. This means that there is some $(a, b) \in (0, 1)$ such that $a_t \rightarrow a$ and $b_t \rightarrow b$ and $d_t \rightarrow 1 - b$ on a subsequence. Hence

$$4 = \lim_{t \rightarrow 0} F_1(a_t, b_t, 1 - a_t, d_t) = \phi(a, b),$$

But then $(a, b) = (1/2, 1/2)$ is the only possible accumulation point. ♠

Corollary 6.5 *Let Σ be any connected component of $L_+(4 - t, 4)$. If t is sufficiently small then Σ intersects the set \mathcal{U} . Moreover, all intersection points have the form (a, b, c, d) with $a, b, c, d \in (2/5, 3/5)$.*

Proof: Let $p = (1/2, 1/2, 1/2, 1/2)$. We compute that $X_G(p) = (2, 2, 2, 2)$. Hence any G -curve through a point sufficiently near p immediately flows into \mathcal{U} . But then by Lemma 6.1 it never hits \mathcal{U} again. These observations apply to points of $\Sigma \cap \mathcal{T}$, by the previous result. ♠

Now we set $g = t$ and $h = (4 - t)/4$. We have

$$N(c, d, t) = (t/4) \times (\lambda(c, d) + t\mu(c, d)), \quad \mu(c, d) = cd(1 + c - d), \quad (59)$$

$$\lambda(c, d) = 2 - 4c + 4c^3 - 2c^4 - 4d + 8cd - 4c^2d + 8c^3d - 4cd^2 - 12c^2d^2 + 4d^3 + 8cd^3 - 2d^4,$$

Lemma 6.6 *For t sufficiently small, V_N is a single arc connecting two distinct points on the open segment σ joining $(1, 0)$ to $(0, 1)$.*

Proof: We compute $\Gamma(1/2, 1/2, t) = -t/4 < 0$. In the square $Q = [2/5, 3/5]^2$ we have $\nabla\lambda = 0$ only at $(1/2, 1/2)$. The point there is a local minimum and the Hessian is positive definite. Moreover, $\lambda(c, d) > 0$ on ∂Q .

Now take $t > 0$ sufficiently small. By continuity $N(c, d, t) > 0$ on ∂Q and $N(c, d, t)$ has a unique local minimum in Q and the value is negative. The location of the minimum converges to $(1/2, 1/2)$ as $t \rightarrow 0$. From this structure and from Corollary 6.5 we see that the solution to V_N is only the one arc which is one half of a nice loop. ♠

As we discussed in connection with Figure 5, the previous result implies that $L_+(4 - t, 4) \cap \mathcal{U}$ is just a single loop for $t > 0$ sufficiently small. Hence $K = 1$ in Theorem 5.1. Now we finish with the goals in this chapter by showing that the nice loop is unique.

Corollary 6.7 *The nice loop is the only component of $L_+ \cap \mathcal{U}$ in all cases. Moreover, ever G -curve in L_+ hits the nice loop.*

Proof: From transversality and the perfect barrier nature of the yellow triangle τ , the set $L_+ \cap \mathcal{U}$ is a union of the nice loop and a finite number of other loops which do not intersect $\mathcal{U}_{ab} \cap \mathcal{U}_{cd}$. Since every G -curve which intersects \mathcal{U} does so at most once and transversely, we see that each of these other loops also contributes to the count of the number of components of L_+ . Since the nice loop already contributes one component, there can be other loops in the intersection.

If some G -curve does not the nice loop then it is in a different component from the component which contains the nice loop. But L_+ is connected, by the Cylinder Theorem, and so this does not happen. ♠

7 Concavity and Intrinsic Boundedness

In this chapter we establish the result in Step 4 of our outline. We show that each level set L_+ of \mathcal{X}_+ is intrinsically bounded and has boundaries which are locally concave everywhere except 2 points.

7.1 The Reversal Lemmas

Our proof is based on results about the action of Δ and $\iota_5 = A\Delta A\Delta A$.

Lemma 7.1 (Reversal I) $\Delta(L_+) = L_+$ and Δ swaps the ends of L_+ .

Proof: A single evaluation, say for the point $(1/4)(2, 1, 2, 1)$, suffices to show that $\Delta(\mathcal{X}_+) \cap \mathcal{X}_+ \neq \emptyset$. Since the component functions of Δ are positive functions we see that $\Delta(\mathcal{X}_+) \subset \mathcal{X}_+$. Since Δ is an involution we $\Delta(\mathcal{X}_+) = \mathcal{X}_+$. Since Δ preserves both invariants we must have $\Delta(L) = L$. Since Δ preserves both invariants and negates the symplectic form, we see that Δ is an isometry of L which reverses the direction of the G -curves. ♠

Let L'_+ denote the subset of L_+ consisting of arcs of G -curves which join points on the nice loop $L_+ \cap \mathcal{U}$ to the backwards end of L_+ . This definition makes sense because each G -curve intersects L'_+ once (and transversely).

Lemma 7.2 (Reversal II) $\iota_5(L'_+) = L'_+$ and ι_5 swaps the ends of L'_+ .

Proof: We compute

$$\iota_5(a, 1 - a, c, d) = (0, \beta, \beta, 0), \quad \beta = \frac{1 - (c + d)}{(c + d) - (c - d)^2}. \quad (60)$$

Note that $\beta > 0$ when our points lie in \mathcal{U}_{ab} .

Conversely, we compute that if $\iota_5(a, b, c, d) = (0, \beta, \gamma, 0)$ then one of the following happens:

$$cd = 0, \quad a + b = 0, \quad a - b + c - d = 0.$$

The last equation comes from the explicit solution

$$a = \frac{d(1 + c - d)}{1 - (c + d)}, \quad b = \frac{c(1 - c + d)}{1 - (c + d)}.$$

In the same way we compute

$$\iota_5(a, b, c, 1 - c) = (\alpha, 0, 0, \alpha), \quad \alpha = \frac{1 - (a + b)}{(a + b) - (a - b)^2}. \quad (61)$$

Again, $\alpha > 0$ when our points lie in \mathcal{U}_{cd} . Conversely, we compute that if $\iota_5(a, b, c, d) = (\alpha, 0, 0, d)$ then one of the following happens:

$$ab = 0, \quad c + d = 0, \quad a - b + c - d = 0.$$

Now let χ be a G -curve of L'_+ . We claim that ι_5 cannot map an interior point of χ to either to $L_+ \cap \mathcal{U}$ to the back end of L_+ . To see this, let \mathcal{H}_{ab} denote the hyperplane given by $a + b = 1$. The same argument as in Lemma 6.1 shows that each G -curve in L_+ intersects \mathcal{H}_{ab} at most once. Hence the interior of χ contains no points of the form (a, b, c, d) with $a + b = 1$. Likewise, the interior of χ contains no points of the form (a, b, c, d) with $c + d = 1$. Furthermore, the interior of χ contains no points where a coordinate is 0 and no points where $a - b + c - d = 0$. The calculations above now show that ι_5 cannot map an interior point of χ to the back end of L_+ . If ι_5 maps some interior point of χ to some point of $L_+ \cap \mathcal{U}$ then (being an involution) ι_5 maps a point of $L_+ \cap \mathcal{U}$ to an interior point of χ . This contradicts Equations 60 or 61.

Call a G -curve χ of L'_+ *good* if $\iota_5(\chi)$ intersects L'_+ . Our claim above combines with the fact that ι_5 is an involution to show that $\iota_5(\chi)$ is precisely a G -curve in L'_+ . If some G -curve in L'_+ is good then by continuity all nearby G -curves in L'_+ are good. Similarly, if we have a sequence of good G -curves in L'_+ then their limit is also good.

This point needs a bit more explanation. If we have a sequence $\{\chi_n\}$ of good G -curves, then the image sequence is just some other sequence of G -curves in L'_+ , from what we have said in the previous paragraph. But then, by transversality, such a sequence has points which lie just a bit inside L'_+ and near $L_+ \cap \mathcal{U}$. The limit of such points belongs to L'_+ .

Now we know that if L'_+ contains a good G -curve then every G -curve of L'_+ is good and hence $\iota_5(L'_+) = L'_+$. Since ι_5 negates the invariant symplectic form, ι_5 must reverse the directions of the G -curves in L'_+ . Hence ι_5 swaps the ends of L'_+ .

It now follows from the same continuity argument that every L'_+ is good provided that one of them is. Finally, we just make an explicit calculation to show that $L'_+(3, 4)$ is good. Hence all the level sets in \mathcal{X}_+ are good. ♠

7.2 The Main Argument

We choose a flat metric on L_+ coming from the integrable structure. Our results below hold for any choice.

Lemma 7.3 *Any level set L_+ in \mathcal{X}_+ is intrinsically bounded.*

Proof: Since $L_+ \cap \mathcal{U}$ is actually a subset of the cylinder L_+ , every point of $p \in L_+$ is less than D_p to every point of $L_+ \cap \mathcal{U}$ for some constant D_p which depends on p . But now we apply ι_5 and conclude that the same boundedness result holds for the backwards end of L_+ . But now we apply Δ and conclude that the same boundedness result holds for the forwards end of L_+ . Putting these results together we see that L_+ is intrinsically bounded. ♠

Lemma 7.4 *Intrinsically, each end of L_+ is a union of 2 concave arcs, meeting at a positive angle at 2 points.*

Proof: In view of the Reversal Lemmas, it suffices to prove this for a neighborhood of $L_+ \cap \mathcal{U}$ in L'_+ . The two curves $L_+ \cap \mathcal{U}_{ab}$ and $L_+ \cap \mathcal{U}_{cd}$ are smooth away from the two points where they meet in $\mathcal{U}_{ab} \cap \mathcal{U}_{cd}$. It suffices to show that these arcs are locally concave with respect to the side that lies in L'_+ . By symmetry, it suffices to prove this for \mathcal{U}_{ab} .

We observe that

$$\frac{X_1 \cdot (1, 1, 0, 0)}{X_2 \cdot (1, 1, 0, 0)} = -\frac{1 - c + d}{1 + c - d}. \quad (62)$$

Thus, if we set

$$Y = \alpha_1 X_1 + \alpha_2 X_2, \quad \alpha_1 = 1 + c - d, \quad \alpha_2 = 1 - c + d, \quad (63)$$

we have

$$\psi = Y \cdot \nabla \phi \Big|_{(a, 1-a, c, d)} = 0. \quad (64)$$

The local convexity in the intrinsic metric is equivalent to the statement that

$$q = Y \cdot \nabla \psi \Big|_{a, 1-a, c, d} \neq 0. \quad (65)$$

Geometrically, what this says is that we travel along the straight line parallel to Y the second derivative of the defining function is nonzero.

Computing the Hessian, we have

$$q = \sum_{i,j} Q_{ij} \alpha_i \alpha_j, \quad Q_{ij} = X_i \cdot \nabla(X_j \cdot h). \quad (66)$$

In other words, we evaluate the quadratic form Q on the vector (α_1, α_2) .

We compute in Mathematica that

$$q = \frac{8a(1-a)(1+c-d)^2(1-c+d)^2(c+d-1)(c+d-(c-d)^2)}{c^2d^2} < 0.$$

Since $c+d < 1$ we have $c+d-1 < 0$. Since $c, d \in (0, 1)$ we have $|c-d| < c+d$. So, the last factor in the numerator is positive. A single plot is enough to show that the positive sign determines concavity rather than convexity with respect to the side of the arc lying in L'_+ . ♠

8 Analytic Continuation

8.1 First Stage

In this chapter we carry out Steps 5 and 6 of our outline. Let L_+ be a level set of \mathcal{X}_+ . Let L denote the level set in \mathbf{R}^4 containing L_+ . We eventually want to see that L is a torus. The level set L is partitioned into various components by the coordinate hyperplanes. One of these components is L_+ . Once again we will use the map ι_5 to help us.

Define

$$(V_1, V_2, V_3, V_4) = dt_5(X_G). \quad (67)$$

Lemma 8.1 $V_1 = V_4 < 0$ for points of $L_+ \cap \mathcal{U}_{ab}$.

Proof: The fact that $V_1 = V_4$ is a direct computation. We will show that $V_1 < 0$. We compute

$$V_1 = \frac{2c(c-2)(1-2c+c^2-2d-2cd+d^2)}{(1+c-d)((c-d)^2-(c+d))} \quad (68)$$

Since $c, d \in (0, 1)$ the only term that can potentially vanish is

$$f = 1 - 2c + c^2 - 2d - 2cd + d^2. \quad (69)$$

The solutions to $f = 0$ are given by $c = 1 + d \pm 2\sqrt{d}$. Since $c \in (0, 1)$ only the $-$ choice is valid. That is

$$c = 1 + d - 2\sqrt{d}. \quad (70)$$

We claim that this variable choice forces $F_1(a, 1-a, c, d) < 0$. To see this we note that this expression is negative when $a = 3/4$ and $c = 1/2$. The value is about -2.343 . Solving the equation $F_1 = 0$ gives the further information that $d = a^2$. This gives $c = (1-a)^2$. But for these choices we see that $G(a, 1-a, c, d) = 0$. Hence, these points do not lie in \mathcal{X}_+ . Since \mathcal{X}_+ is connected, and since the nice loops $L_+ \cap \mathcal{U}_{ab}$ vary continuously for level sets in \mathcal{X}_+ , it follows from continuity that we never have $F_1 > 0$ when $c = 1 + d - 2\sqrt{d}$. This proves $V_1 < 0$, as desired. ♠

Recall that the G -curves are not defined at the coordinate hyperplanes. However, it may happen that there are 2 different G -curves γ_1 and γ_2 and

a point p such that p is the forwards endpoint of γ_1 and the backwards endpoint of γ_2 . We say that γ_1 and γ_2 are *analytic partners* if there is a regular analytic curve $\gamma = \gamma_1 \cup \gamma_2 \cup p$. Here *regular* means that it has an analytic parametrization with nonzero derivative everywhere. We call p the *join point* for (γ_1, γ_2) .

We say that two disjoint components L_1, L_2 of L are *analytic partners* if all but finitely many common accumulation points of L_1 and L_2 are join points for a pairs of analytic partners. Each pair of partners has one G -curve in L_1 and one in L_2 .

Lemma 8.2 L_+ has 2 disjoint analytic partners across its back end.

Proof: We will show that L_+ is joined to an analytic partner across the subset of accumulation points of the form $(0, b, b, 0)$. Here $b \in [0, 1]$. We omit the case $b = 0$ from discussion. (This is why we throw away finitely many accumulation points.) By symmetry, L_+ is joined to another analytic partner across the subset of accumulation points of the form $(a, 0, 0, a)$ with $a \in [0, 1]$. These two analytic partners are distinct because the coordinates of points in them have different signs.

Consider a small open neighborhood U of $L_+ \cap \mathcal{U}_{ab}$. We have already shown that ι_5 carries $U \cap L'_+$ to a neighborhood of the back end of L_+ that accumulates on points of the form $(0, b, b, 0)$. Now we look at the image of $U - L'_+$, namely the other side of $L_+ \cap \mathcal{U}$, under ι_5 . We argue that ι_5 carries this set into the same component of L , and that this component is an analytic partner. This comes down to a calculation.

The map ι_5 is well-defined and analytic in U . Hence the image of a G -curve in L is analytic. The subset of the image not contained in the coordinate hyperplanes is a union of G -curves, because $\iota_5(X_G) = -X_G$ whenever the domain and range are not in the coordinate hyperplanes.

We define $(V_1, V_2, V_3, V_4) = d\iota_5(X_G)$, as above. We have already proved that $V_1 = V_4 < 0$ when we are doing the computation based at a point of $L_+ \cap \mathcal{U}_{ab}$. Thus, we see that when U is sufficiently small, points of L_+ on the other side of $L_+ \cap \mathcal{U}_{ab}$ from L'_+ map into the subset of \mathbf{R}^4 consisting of points (a', b', c', d') where $a', d' < 0$ and $b', c' > 0$. This remains true as we move around in $L_+ \cap \mathcal{U}_{ab}$ as long as we stay away from the point that ι_5 maps to $(0, 0, 0, 0)$. Being connected, $\iota_5(U - L'_+)$ lies in one component of L . ♠

8.2 Second Stage

Recall that $A(a, b, c, d) = (-b, -a, -d, -c)$. This is an everywhere defined linear map of \mathbf{R}^4 . Define

$$L_- = A(L_+). \quad (71)$$

The coordinates of all points on L_- are negative. Hence L_+ and L_- are disjoint. On the other hand, both L_+ and L_- have $(0, 0, 0, 0)$ as an accumulation point. Since L_+ has 2 disjoint analytic partners across its back end, L_- has 2 disjoint analytic partners across its front end.

Lemma 8.3 *The 2 back-end analytic partners of L_+ coincide with the 2 front-end analytic partners of L_- .*

Proof: Since every component of L is a smooth surface, and since the analytic partners involved of L_+ and L_- vary continuously with the parameters, and since the space of level sets of \mathcal{X}_+ is connected, it suffices to show for some choice of parameters that the lemma is true.

Let \mathcal{H}_{ab} be the hyperplane given by $a+b=1$. We have $\mathcal{U}_{ab} \subset \mathcal{H}_{ab}$. Define $\mathcal{V}_{ab} = \mathcal{H}_{ef} - \mathcal{U}_{ab}$. Likewise define \mathcal{H}_{cd} and \mathcal{V}_{cd} . Say that the level set L is *clean* if $\gamma_{ab} = L_+ \cap \mathcal{H}_{ab}$ and $\gamma_{cd} = L_+ \cap \mathcal{H}_{cd}$ are closed loops.

The same proof as in the previous chapter shows that $L(4-t, 4)$ is clean for $t > 0$ sufficiently small. In this case we have a small cylinder passing transversely through 2 transverse hyperplanes. From this picture we see that γ_{ab} and γ_{cd} intersect exactly twice. Figure 6 shows schematically what this looks like in the flat structure. The left and right boundaries are supposed to be identified by translation.

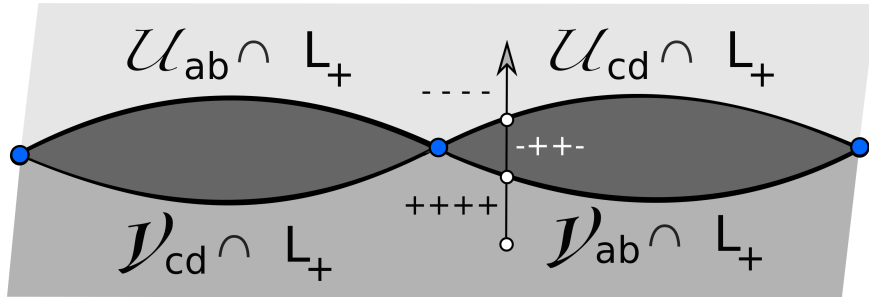


Figure 6: The cylinder L_+ near γ_{ab} and γ_{cd} .

The various boundary curves are always locally convex but their exact shape depends on the parameters. The reader should compare Figure 6 with Figure 3 in §3.6. The left and right sides are meant to be identified.

The same analysis as in the previous section shows that $d\iota_5$ is nonsingular on points of $L_+ \cap \mathcal{H}_{ab}$. We start with a G -curve χ in L_+ that is near one of the points where L_+ intersects $\mathcal{H}_{ab} \cap \mathcal{H}_{cd}$. Figure 6 shows what this curve looks like intrinsically. Given the properties of ι_5 , the image $\iota_5(\chi)$ is a regular analytic curve with 2 break points, one an accumulation point of the back end of L_+ and the second one an accumulation point on the front end of L_- .

Figure 6 indicates the signs of the coordinates of points along $\iota_5(\chi)$. Once all the coordinates of $\iota_5(\chi)$ are negative, they must lie in L_- because the level set L has only one connected component on $A(\mathcal{X}_-)$. This follows from the Cylinder Theorem and symmetry. Thus, the existence of $\iota_5(\chi)$ shows that one and the same component is a back-end analytic partner of L_+ and a front-end analytic partner of L_- . A similar argument works for the other pair of analytic partners. ♠

Let D_1 and D_2 denote the two back-end analytic partners of L_+ . As we have just seen D_1 and D_2 are also front-end analytic partners of L_- .

The analysis above works even for the G -curves which go through the points of $L_+ \cap \mathcal{H}_{ab} \cap \mathcal{H}_{cd}$. In this case ι_5 maps these G -curves to regular analytic curves which pass directly from L_+ to L_- . There are 2 such G -curves, corresponding to the 2 intersection points on the nice loop discussed in the previous chapter. From all this structure, we see that the development of $L_+ \cup L_- \cup D_1 \cup D_2$ looks like Figures 3 and 6. The two cylinders L_+ and L_- abut at two cusp points and D_1, D_2 fit in between. The boundaries of D_1 and D_2 are convex because the boundaries of L_+ and L_- are concave away from the two cusps.

Lemma 8.4 $A(D_1) = D_1$ and $A(D_2) = D_2$.

Proof: It follows from the fact that $A(L_\pm) = L_{mp}$ that $A(D_1 \cup D_2) = D_1 \cup D_2$. One of the disks D_1 has accumulation points of the form $(a, 0, 0, a)$ for $a > 0$ and $(0, -b, -b, 0)$ for $a, b > 0$. The other disk D_2 has accumulation points of the form $(0, b, b, 0)$ and $(-a, 0, 0, -a)$ for $a > 0$. Given that $A(a, b, c, d) = (-b, -a, -d, -c)$ we see that $A(D_1)$ has accumulation points of the same kind that D_1 does. Hence $A(D_1) = D_1$. Likewise $A(D_2) = D_2$. ♠

8.3 Third Stage

Let $\iota_3 = A\Delta A$. In this section we prove that L_+ has 2 disjoint analytic partners across its front end. The proof uses ι_3 much like the argument in Stage 1 used ι_5 .

Lemma 8.5 Δ is well-defined and nonzero on $D_1 \cup D_2$.

Proof: The equation for Δ is given in Equation 12.

Since D_1 is an analytic partner of the back end of L_+ there are points $(a, b, c, d) \in D_1$ satisfying $|a - b| < 1$. Given that a and b have opposite signs, this forces $|a| + |b| < 1$ as well. Likewise $|c| + |d| < 1$. The denominators of the coordinates of $\Delta(a, b, c, d)$ vanish only if

$$d = -\frac{(1+a)(1+c)}{b}.$$

Since $|a| + |b| < 1$ we have $|1+a|/|b| > 1$. Thus $|d| > 1$. This is a contradiction.

Here are the solutions to the equation $\Delta(a, b, c, d)_k = 0$. In other words, we set the k th term to 0 and solve.

1. $b = 0$ or $c + d = -1$.
2. $d = 0$ or $bd + ac = -b - c$.
3. $a + b = -1$ or $d = 0$.
4. $b = 0$ or $ac + bd = -a - d$.

Our constraints above rule out all these possibilities. To explain one of the two non-obvious ones, suppose $bd + ac = -b - c$. Then

$$d = \frac{-b - c - ac}{b} = -1 + \frac{c(-1 - a)}{b}. \quad (72)$$

There are two cases and in either case $|a| < 1$ and $b/c > 0$. This means that the second term on the right side of Equation 72 is negative and $d < -1$. This is a contradiction. The other non-obvious impossibility has the about the same treatment. ♠

Lemma 8.6 $\Delta(D_1)$ and $\Delta(D_2)$ are front-end analytic partners of L_+ .

Proof: By Lemma 8.5, the sets $\Delta(D_1)$ and $\Delta(D_2)$ are contained in components of L . The map Δ is not defined on ∂D_1 or ∂D_2 but the last two coordinates of $\Delta(a, 0, 0, a)$ are defined and the first two coordinates of $\Delta(0, b, b, 0)$ are well defined. We have

$$\Delta(a, 0, 0, a) = (*, *, 1, 0), \quad \Delta(0, b, b, 0) = (1, 0, *, *). \quad (73)$$

The starred components would require more information to determine. However, the above equations imply that Δ maps the boundaries of D_1 and D_2 into the coordinate hyperplanes. Hence $\Delta(D_1)$ and $\Delta(D_2)$ are precisely components of L .

Now we want to see that $\Delta(D_1)$ and $\Delta(D_2)$ are analytic front-end partners of L_+ . We cannot directly compute the value of Δ on the boundary of D_j but we recall that ι_5 maps $L_+ \cap \mathcal{U}$ to the back end of L_+ , the very spot we are interested in. When we compute $\Delta \circ \iota(a, b, c, d)$ we get an expression of the form

$$\left(*, *, \frac{N_3}{D_3}, \frac{N_4}{D_4} \right) \quad (74)$$

We write things this way to make sure we are never only dealing with polynomials. Then $b = 1 - a$ we find that (as expected) the first two values are 1 and 0. We also have

$$N_3 = -2a^2d(1-a)^3(1+c-d)^3(1-c+d)(c^2 - 2cd - 2c + d^2 - 2d + 1).$$

$$D_3 = -2a^2c(1-a)^3(1+c-d)^2(1-c+d)^2(c^2 - 2cd - 2c + d^2 - 2d + 1).$$

Hence we have the well defined value

$$\frac{N_3}{D_3} = \frac{d(1+c-d)}{c(1-c+d)}. \quad (75)$$

Similarly,

$$\frac{N_3}{D_3} = \frac{1-(c+d)}{c(1-c+d)}. \quad (76)$$

All the factors in N_3, N_4, D_3, D_4 are nonzero except perhaps the last factor. But these last factors appear identically in the numerator and the denominator. Hence $\Delta \circ \iota$ has an analytic extension to $L_+ \cap \mathcal{U}$. Moreover, $\Delta \circ \iota$ maps one side of $L_+ \cap \mathcal{U}$ to a neighborhood of the front end of L_+ and the other side to a neighborhood of $\Delta(D_1) \cup \Delta(D_2)$. ♠

8.4 Fourth Stage

Let D_3, D_4 be the front-end analytic partners of L_+ and let D_5, D_6 be the back-end analytic partners of L_- . In this section we will identify M as the common analytic partner to all of D_3, D_4, D_5, D_6 .

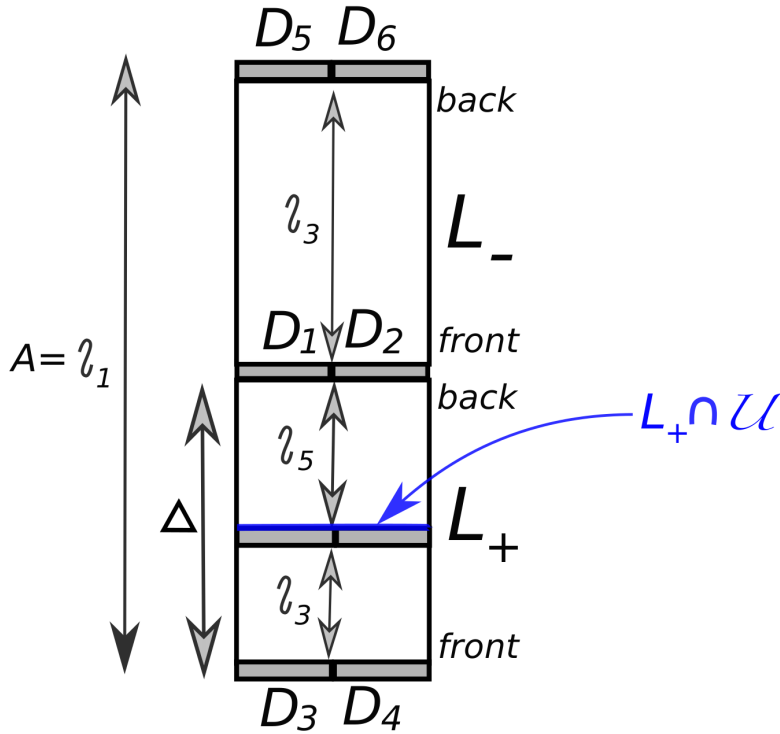


Figure 8: A schematic picture in the clean case.

Figure 8 shows a summary of the action of the various involutions we have shown so far, and one additional one. We represent our disks as shaded rectangles and the cylinders as white rectangles. This picture is combinatorially accurate but geometrically misleading. For instance, $D_1 \cup D_2$ has 2 pinch points. It is not really a solid annulus. Also, $\iota_5(D_1 \cup D_2)$ is only contained in L_+ in the clean case. In general, this set can stick out the front end of L_+ .

For our final cylinder, we define

$$M = \iota_3(L'_+). \quad (77)$$

Lemma 8.7 *M is a component of L.*

Proof: We compute

$$\iota_3(a, 1 - a, c, d) = \left(\frac{c(1 - c + d)}{d(1 + c - d)}, \frac{(c + d) - 1}{d(1 + c - d)}, 1, 0 \right). \quad (78)$$

The action of $\iota_3(A)$ on the other end of L'_+ is the same as the action of Δ on one end of $D_1 \cup D_2$, which we have already discussed. This ι_3 maps the ends of L'_+ into the coordinate hyperplanes.

To finish the proof we just have to see that ι_3 is well-defined and nonzero on L'_+ . We will show this for all of L_+ . If a, b, c, d are nonzero, the denominators of these expressions vanish only when

$$c = -\frac{(1 - b)(1 - d)}{a}.$$

The expression on the right is negative for points in L_+ , so the denominator never vanishes. Aside from points in the coordinate hyperplanes, the only choices which make one of the numerators vanish is

$$c = \frac{a + d - bd}{a} > 1, \quad d = \frac{b + c - ac}{b} > 1. \quad (79)$$

These values do not occur in L_+ . ♠

Lemma 8.8 *M is an analytic partner of D_3 and of D_4 .*

Proof: We can view $\iota_5(D_1 \cup D_2)$ as a union of analytic partners for L'_+ , even though there is no actual barrier here. We then compute

$$\iota_3 \circ \iota_5(D_1 \cup D_2) = \Delta \circ A(D_1 \cup D_2) = \Delta(D_1 \cup D_2) = D_3 \cup D_4.$$

This M lies on the other side of $D_3 \cup D_4$ from L_+ . Moreover, one end of M , namely $\iota_3(L_+ \cap \mathcal{U})$ has common accumulation points with the far end of $D_3 \cup D_4$. To see that M is really an analytic partner to these disks, we let

$$(W_1, W_2, W_3, W_4) = d\iota_3(X_G).$$

We compute

$$W_4 = \frac{4c(2-c)}{1+c-d} > 0.$$

From this we conclude that the G -curves exiting $D_3 \cup D_4$ on the far side, the side opposite the one abutting L_+ , are joined to G -curves in M by regular analytic arcs. This shows that M is an analytic partner of each of D_3 and D_4 . ♠

Lemma 8.9 *M is an analytic partner of D_5 and of D_6 .*

Proof: Since $L_- = A(L_+)$, the map $\iota_3 = A\Delta A$ acts on L_- just as Δ acts on L_+ . Thus $\iota_3(D_1 \cup D_2) = D_5 \cup D_6$. The rest of the proof is very much like that in Lemma 8.6. The main point is that want to understand the action of Δ on the back end of L'_+ , but this is the same as the action of $\iota_3\iota_5$ on $L_+ \cap \mathcal{U}$. Working similarly to Lemma 8.6 we find that

$$\iota_3 \circ \iota_5(a, 1-a, c, d) = \delta \circ A(a, b, c, d) = \left(\frac{1-(c+d)}{d(1+c-d)}, \frac{-1+c-d}{d(1+d-c)}, 0, -1 \right). \quad (80)$$

The rest of the argument is the same as in Lemma 8.6.

8.5 Behold the Torus

The components of L we have described above fit together as in Figure 3 to make a flat torus. Call this object \widehat{L} . It might be the case that L has components other than the ones comprising \widehat{L} , but this is irrelevant for our proof. (I think that there are no other components.)

Lemma 8.10 $A(\widehat{L}) = \widehat{L}$.

Proof: We have already seen that the action of A permutes all the pieces we have defined except perhaps for M . But A swaps the union $D_3 \cup D_4$ with the union $D_5 \cup D_6$ and preserves analytic partnership. Also $A(L_\pm) = L_\mp$. Hence $A(M) = M$. Since A permutes all the pieces of L we have $A(\widehat{L}) = \widehat{L}$. ♠

Lemma 8.11 *The action of Δ on L induces an isometric action $\widehat{\Delta}$ on \widehat{L} whenever Δ on \widehat{L} . In short, $\widehat{\Delta}(\widehat{L}) = \widehat{L}$ and $\widehat{\Delta}$ extends the action of Δ .*

Proof: Since everything in sight is an intrinsic isometry we just have to prove that Δ maps all the components of L involved in \widehat{L} back into \widehat{L} . Let us examine all the pieces. We already know that

$$\Delta(L_+) = L_+ \subset \widehat{L}.$$

We also already know that

$$\Delta(D_1 \cup D_2) = D_3 \cup D_4 \subset \widehat{L}.$$

Since $L_- = A(L_+)$ and $A(\widehat{L}) = \widehat{L}$, we can show that $\Delta(L_-) \subset \widehat{L}$ by showing that $\iota_3(L_+) \subset \widehat{L}$. We have

$$\iota_3(L_+) = \iota_3(L'_+) \cup \iota_3(L''_+) \cup \iota_3 \circ \iota_5(D_1 \cup D_2) = M \cup L''_+ \cup D_3 \cup D_4 \subset \widehat{L}.$$

Hence $\Delta(L_-) \subset \widehat{L}$.

We have

$$\Delta(D_3 \cup D_4) = D_1 \cup D_2 \subset \widehat{L}.$$

Now we want to show that $\Delta(D_5 \cup D_6) \subset \widehat{L}$. Since $A(\widehat{L}) = \widehat{L}$ and A swaps $D_3 \cup D_4$ with $D_5 \cup D_6$, it suffices to show that $\iota_3(D_5 \cup D_6) \subset \widehat{L}$. But

$$\iota_3(D_5 \cup D_6) = D_1 \cup D_2 \subset \widehat{L}.$$

This does the job.

Finally, since Δ is an involution, we have

$$\Delta(M) = L'_+ \subset \widehat{L}.$$

This completes the proof. ♠

Now we know that the group $\langle A, \widehat{\Delta} \rangle$ gives an isometric action on \widehat{L} extending the action of $\langle A, \Delta \rangle$ on L . Numerically we can see that there are no other components of L , but this is irrelevant for our proof. If we pick a point $p \in L_+$, then the orbit of p under $T_3 = (A\Delta)^2$ remains in \widehat{L} forever or else T_3 is undefined for some iterate.

This completes the proof sketched in §3.6 and thereby completes the proof of Theorem 1.2 for centrally symmetric 8-gons which are neither inscribed nor circumscribed. In the next chapter we take care of the inscribed and circumscribed case.

9 The Inscribed and Circumscribed Cases

In this chapter we complete the proof of Theorem 1.2, then prove Theorem 1.3. For theorem 1.2 it suffices by duality just to consider \mathcal{I}^* , the set of circumscribed centrally symmetric 8-gons.

We work with the functions defined in Equation 15. The points in \mathcal{I}^* satisfy $g_{ab}^* + g_{cd}^* = 0$. A calculation shows that T_3 preserves this condition. Hence \mathcal{I}^* is T_3 -invariant.

Let Π_k denote the plane of points where $g_{ab}^* = -g_{cd}^* = 2k$. A point in this plane is given by $(x+k, x-k, y-k, y+k)$. The space \mathcal{I}^* is partitioned into these planes. We have $T_3 = (A\Delta)^2$, and $A\Delta$ swaps \mathcal{I} and \mathcal{I}^* . Let

$$h = -g_{ab} \circ (A\Delta) = \frac{b-c-ac+bc-c^2-ac^2+cd+acd-bcd+bd^2}{bd}. \quad (81)$$

Define

$$L(k, \ell) = \Pi_k \cap h^{-1}(\ell). \quad (82)$$

Lemma 9.1 T_3^4 preserves $L(k, \ell)$ and the action is conjugate to a linear fractional transformation acting on the Riemann sphere.

Proof: A direct calculation shows that $T_3^2(\Pi_k) = \Pi_{-k}$. Hence $T_3^4(\Pi_k) = \Pi_k$. A direct calculation shows that when $p \in \Pi_k$ we have

$$\psi \circ T_3(p) = -i\psi(p), \quad \psi(a, b, c, d) = h(a, b, c, d) + ih(b, a, d, c). \quad (83)$$

Hence $T_3^4(L(k, \ell)) = L(k, \ell)$.

The restriction of h to Π_k is given by

$$h(x+k, x-k, y-k, y+k) = \frac{4k^3 - x + y - 4kxy}{(k-x)(k+y)}. \quad (84)$$

$L(k, \ell)$ satisfies the equation we get by setting the right hand side of Equation 84 to ℓ and clearing denominators. This gives a quadratic equation:

$$(\ell - 4k)xy + (1 + k\ell)x - (1 + k\ell)y - (4k^3 - k^2\ell). \quad (85)$$

As a projective variety in the \mathbf{CP}^2 , this curve is a sphere. Thus, the restriction of T_3^4 to $L(k, \ell)$ is a linear fractional transformation when this sphere is identified with the Riemann sphere *via* a biholomorphic map. ♠

We let $\phi_{k,\ell}$ denote the extension of $T_3^4|_{L(k,\ell)}$ to the Riemann sphere, after $L(k,\ell)$ is identified with the Riemann sphere. The map T_3^4 is perhaps not defined at all points of the Riemann sphere $\mathbf{C} \cup \infty$. But, wherever T_3^4 is defined, it agrees with the linear fractional transformation $\phi_{k,\ell}$. Note that $L(k,\ell)$ contains convex points if and only if $|k| < 1/2$ and $|\ell| < 2$.

Lemma 9.2 *If $|k| < 1/2$ and $|\ell| < 2$ then $\phi_{k,\ell}$ is a hyperbolic linear transformation with precisely 2 fixed points. The fixed points cannot correspond to convex 8-gons which are not Poncelet.*

Proof: In $L(k,\ell)$ we can directly solve the equation $\phi_{k,\ell}(z) = z$ for x and y . There are (formally) two solutions $(x_0, -y_0)$ and $(y_0, -x_0)$, where

$$x_0 + y_0 = \frac{2(4k - \ell)(k\ell - 1)}{(2 + \ell)(2 - \ell)}, \quad x_0 y_0 = \frac{-2 - 4k + 4k\ell - k^2 \ell^2}{(2 + \ell)(2 - \ell)}. \quad (86)$$

The polynomial $t^2 - (x_0 + y_0)t + x_0 y_0$ has discriminant

$$D = 4(1 + 4k^2 - 2k\ell)((8 - \ell^2) - 8k\ell + 4(k\ell)^2). \quad (87)$$

The number of solutions is 0, 1, 2 according as D is negative, zero, positive. D is positive when $|k| < 1/2$ and $|\ell| < 2$ and thus we get 2 distinct real solutions. A calculation shows that $g_{ab} + g_{cd} = 0$ for the solutions. Since $g_{ab}^* + g_{cd}^* = 0$ as well, any non-degenerate fixed point is Poncelet.

The map $\phi_{k,\ell}$ has 2 real fixed points and preserves the circle in $\mathbf{C} \cup \infty$ corresponding to the real points of $L(k,\ell)$. Hence this map is either hyperbolic or elliptic of order 2. Since the set where $|k| < 1/2$ and $|\ell| < 2$ is connected, the same option always occurs. A single evaluation is enough to establish that the hyperbolic option occurs. ♠

Suppose now that we have a convex point $\xi \in L(k,\ell)$ which is convex but not Poncelet. By the previous result, the forward $\phi_{k,\ell}$ iterates of ξ converge to one fixed point and the backwards iterates converge to the other. The fixed points of $\phi_{k,\ell}$ have the form $(x_0, -y_0)$ and $(y_0, -x_0)$. Since these are distinct, there is at least one negative number amongst the coordinates of these points. But this means that either some iterate of T_3^4 is undefined on ξ or else some iterate of T_3^4 on ξ has a negative coordinate. In either case, all iterates of ξ under T_3^4 cannot be convex. This completes the proof of Theorem 1.2. Now we turn towards the proof of Theorem 1.3.

Lemma 9.3 \mathcal{CI}^* is forward T_3 -invariant.

Proof: Let P_1, \dots, P_8 be the points of ξ . Let $\sigma_j = \overline{P_j P_{j+3}}$. Suppose that $\sigma_1, \sigma_2, \sigma_3$ are coincident. That is, the lines extending them intersect at a single point. Then the points P_1, \dots, P_6 are the vertices of an inscribed hexagon, by the converse of Brianchon's Theorem. This is impossible for a circumscribed 8-gon: $P_1 P_6$ is not tangent to the circumscribing ellipse.

Now we know that $\sigma_1, \sigma_2, \sigma_3$ are never coincident. By symmetry the same goes for all σ_i . Hence, as we vary $P \in \mathcal{CI}^*$ the image $T_3(P)$ is never degenerate. When P is regular, $T_3(P)$ is convex. So, by continuity this holds for all $P \in \mathcal{CI}^*$. Also, $T_3(\xi)$ is again circumscribed because \mathcal{I}^* is T_3 -invariant. ♠

Lemma 9.4 If $|k| < 1/2$ and $|\ell| < 2$ then one of the fixed points of $\phi_{k,\ell}$ is a convex Poncelet 8-gon and the other point is a star-convex Poncelet 8-gon.

Proof: If the point (a, b, c, d) represents a convex Poncelet polygon, then the point $(-a, -b, -c, -d)$ represents a star-convex Poncelet polygon. If $\phi_{k,\ell}$ fixes (a, b, c, d) then, by symmetry, it also fixes $(-a, -b, -c, -d)$. Hence, if one fixed point is convex Poncelet then the other is star-convex Poncelet. We just have to show that one of the fixed points is a convex Poncelet 8-gon.

One of the fixed points (a, b, c, d) is the limit of convex 8-gons in $L(k, \ell)$. This gives us

$$|a - b| = |k| < 1, \quad |c - d| = |\ell| < 2, \quad a + b \geq 1, \quad c + d \geq 1.$$

If $a + b = 1$ then $g_{ab}(a, b, c, d) = 2$. But then $g_{cd}(a, b, c, d) = -2$. This is not possible for a finite pair (c, d) . Hence $a + b > 1$. Likewise $c + d > 1$. Hence (a, b, c, d) gives a nontrivial convex 8-gon which is Poncelet. By Lemma 9.2. ♠

Since the set $\{k, \ell \mid |k| < 1/2, |\ell| < 2\}$ is connected and since $\phi_{k,\ell}$ is always hyperbolic, the convex Poncelet 8-gon is either always attracting or always repelling. A single evaluation is enough to see that the attracting case holds.

Suppose now that $\xi \in \mathcal{CI}^*$. Then $T_3^n(\xi)$ is convex and circumscribed for all $n \geq 0$. In particular, $T_3^{4n}(\xi) = \phi_{k,\ell}(\xi)$. From what we have said above, we see that $T_3^{4n}(\xi)$ converges to the affine equivalence class of a star-convex Poncelet 8-gon. But this limit is fixed by T_3 . Hence, by continuity, $T_3^{4n+m}(\xi)$ converges to the same limit for all $m = 0, 1, 2, 3$. This proves the first statement in Theorem 1.3. The second statement has a very similar proof.

References

- [1] M. Glick, *The Limit Point of the Pentagon Map*, International Mathematics Research Notices 9 (2020) 2818–2831
- [2] M. Glick, *The pentagram map and Y-patterns*, Adv. Math. **227**, 2012, 1019–1045.
- [3] M. Gekhtman, M. Shapiro, S. Tabachnikov, A. Vainshtein, *Higher pentagram maps, weighted directed networks, and cluster dynamics*, Electron. Res. Announc. Math. Sci. **19** 21012, 1–17
- [4] L. Halbeisen and N. Hungerbühler, *A Simple proof of Poncelet’s Theorem (on the occasion of its bicentennial)* Amer. Math. Monthly, **122** No. 6, 2015, pp 537-551
- [5] A. Izosimov, *The pentagram map, Poncelet polygons, and commuting difference operators*, arXiv 1906.10749 (2019)
- [6] B. Khesin, F. Soloviev *Integrability of higher pentagram maps*, Mathem. Annalen. (to appear) 2013
- [7] Wolfram Research Inc., *Mathematica*, Wolfram Programming Lab, Champaign, IL (2021)
- [8] G. Mari Beffa, *On Generalizations of the Pentagon Map: Discretizations of AGD Flows*, arXiv:1303.5047, 2013
- [9] G. Mari Beffa, *On integrable generalizations of the pentagram map* arXiv:1303.4295, 2013
- [10] Th. Motzkin, *The pentagon in the projective plane, with a comment on Napier’s rule*, Bull. Amer. Math. Soc. **52**, 1945, 985–989.
- [11] V. Ovsienko, R. Schwartz, S. Tabachnikov, *The pentagram map: A discrete integrable system*, Comm. Math. Phys. **299**, 2010, 409–446.
- [12] V. Ovsienko, R. Schwartz, S. Tabachnikov, *Liouville-Arnold integrability of the pentagram map on closed polygons*, to appear in Duke Math. J.
- [13] B. Rodin and S. Sullivan, *The convergence of circle packings to the Riemann mapping*, J. Diff. Geom. 26 (1987) 349–360

- [14] R. Schwartz, *The pentagram map*, Experiment. Math. **1**, 1992, 71–81.
- [15] R. Schwartz, *Discrete monodromy, pentagrams, and the method of condensation*, J. of Fixed Point Theory and Appl. **3**, 2008, 379–409.
- [16] R. Schwartz, *The Poncelet Grid*, Advances in Geometry 7 (2006)
- [17] R. Schwartz, *A Textbook Case of Pentagon Rigidity*, preprint (2021)
- [18] R. Schwartz, S. Tabachnikov, *Elementary surprises in projective geometry*, Math. Intelligencer (2010)
- [19] J. Silverman, *The arithmetic of dynamical systems*, Springer
- [20] F. Soloviev *Integrability of the Pentagon Map*, Duke Math J.
- [21] M. Weinreich, *The Algebraic Dynamics of the Pentagon Map*, (2021)
arXiv: 2104.06211